AD-A193 428 IN - FLIGHT LOAD MEASUREMENTS OF THE ROBOT - X CANARDS (U) DEFENCE RESEARCH ESTABLISHMENT SUFFIELD RALSTON (ALBERTA) S G PENZES FEB 88 DRES-SM-1191 1/1

UNCLASSIFIED F/G 1/1 NL

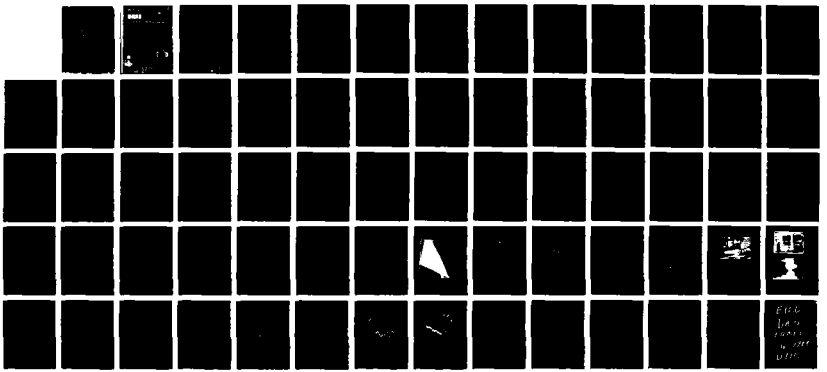

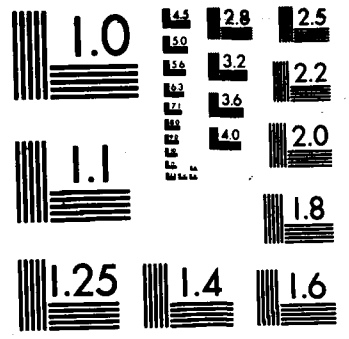

National Défense
Defence nationale

UNCLASSIFIED

DRES

SUFFIELD MEMORANDUM

NO. 1191

IN – FLIGHT LOAD MEASUREMENTS OF THE ROBOT – X CANARDS (U)

by

S. Penzes

PCN 031SE

February 1988

DEFENCE RESEARCH ESTABLISHMENT SUFFIELD, RALSTON, ALBERTA

DEFENSO PER SCIENTIAM

Canada

UNCLASSIFIED

DEFENCE RESEARCH ESTABLISHMENT SUFFIELD

RALSTON, ALBERTA

SUFFIELD MEMORANDUM NO. 1191

IN-FLIGHT LOAD MEASUREMENTS OF THE ROBOT-X CANARDS (U)

by

S. Penzes

PCN 031SE

UNCLASSIFIED

DEFENCE RESEARCH ESTABLISHMENT SUFFIELD
RALSTON, ALBERTA

SUFFIELD MEMORANDUM NO. 1191

IN-FLIGHT LOAD MEASUREMENTS OF THE ROBOT-X CANARDS (U)

by

S. Penzes

ABSTRACT

The strain gauge system implemented in one of the ROBOT-X canards is described. The system is designed to measure lift, drag and torque. The description includes design considerations, calibration procedures and data reduction techniques. Data are presented from an early ROBOT-X flight test.

ACKNOWLEDGEMENT

The support of Mr. J. Vesso throughout this project is greatly appreciated. His experience in the design and installation of strain gauge circuits was invaluable. The efforts of Mr. D. Benson and Mr. J. Smith during the calibration and interfacing with the telemetry subsystem are also greatly appreciated.

TABLE OF CONTENTS

LIST OF FIGURES

LIST OF FIGURES (cont'd)

LIST OF TABLES

DEFENCE RESEARCH ESTABLISHMENT SUFFIELD
RALSTON, ALBERTA

SUFFIELD MEMORANDUM NO. 1191

IN-FLIGHT LOAD MEASUREMENTS OF THE ROBOT-X CANARDS (U)

by

S. Penzes

1.0 INTRODUCTION

ROBOT-X is a rocket-boosted aerial target designed to simulate a variety of air threats for use in exercising air defence weapon systems. Its configuration is illustrated in Figures 1, 2 and 3. The airframe is made almost entirely of composite materials, with a length of 3.4 m and wing span of 2.4 m. Propulsion is by means of nineteen CRV-7 rocket motors, fired in pre-programmed stages. A wide variety of flight profiles may be achieved via a programmable microprocessor-based digital autopilot. The target is recovered by a parachute system. Flight tests conducted during 1986 have established the technical soundness of the ROBOT-X concept.

The ROBOT-X airframe is unique in terms of both aerodynamic configuration and structural design. Consequently, there is considerable research value in obtaining full scale measurements of aerodynamic

loads on key members. The canards are a natural choice for such measurements, because they are of primary importance from a control standpoint (pitch and altitude) and represent one of the most unique aspects of the ROBOT-X configuration.

This memorandum describes the strain gauge system implemented in one of the ROBOT-X canards to measure lift, drag and torque. The description includes design considerations, calibration procedures and data reduction techniques. Data are presented from an early ROBOT-X flight test.

2.0 DESIGN APPROACH

The objective is to produce relevent aerodynamic data for the canards from data acquired during the fl ghts of ROBOT-X. This objective was accomplished in four stages.

1) The design of the on board measurement system. This design utilized three decoupled strain gauge bridges. These bridges produce output which is directly proportional to the instantaneous lift, drag and torque on the canard.

2) The determination of a cross talk correlation matrix from preflight testing of the canard with known loads. This matrix is used to mathematically remove the influence of cross channel systematic errors from the inflight data.

3) The implementation of a preflight shunt calibration methodology. This calibration is used to electronically simulate loads on the canard. The primary purpose is to verify that

the on board signal conditioning is performing as designed.

4) The implementation of a post flight analysis method that converts the flight induced strain measurements to meaningful aerodynamic loading.

3.0 STRAIN GAUGE CONFIGURATION

The canard configuration and internal structure are shown in Figure 4. The main structural member is an aluminum shaft at the 25% chord line. The shaft is set in an instant set polymer (ISP) casting, from which pockets are machined to reduce the weight and rotational inertia. The casting is covered with fibreglass.

In keeping with normal aeronautical practice, the principal loads acting on the canard are considered to be lift, drag and pitching moment. Measurement of the strains produced by these loads is accomplished by mounting strain gauges on the shaft as shown in Figures 5 and 6. This particular configuration was chosen for the following reasons.

1) If gauges #1 and #2, used to measure lift, are wired into adjacent arms of the Wheatstone bridge (see Figure 7) then:
   - the effects of axial load, as would be introduced by side forces due to high roll rates, are cancelled;
   - the effects of thermal coefficient mismatch between the shaft and the strain gauges are cancelled;

- the output of the bridge is twice that of a single active arm bridge; and
- the effects of temperature induced strains are cancelled provided it is assumed that the temperature at the cross section is uniform.

2) The same arguments hold for the drag measurement bridge (gauges #3 and #4).

3) The torque bridge is also thermally compensated and provides four times the output of a single active arm bridge.

With the gauges mounted on the shaft as shown in Figure 6 and considering that the whole assembly (canard surface and shaft) rotates, it can be said that this configuration provides information in the "canard" co-ordinate system. Conversion to the "body" coordinate system is easily accomplished through a coordinate transformation based on the sweepback angle of the canard (θ_s), the canard incidence angle (α_c, measured with a potentiometer in the servo motor) and vehicle flight path angle (γ, estimated by the autopilot). This procedure is described in Section 6.

4.0 STATIC CALIBRATION PROCEDURE

If the measured quantities of strain are to be used to derive an estimate of the aerodynamic forces, consideration must be given to the systematic errors due to factors such as:

- gauge installation misalignment,
- the fact that strain gauges actually provide an average strain over the active grid area, and
- the strain gradient produced by the curvature of the substrate to which the gauges are applied.

It was determined that a calibration procedure should be established which, combined with some mathematical compensation, would provide a means to compensate for these systematic errors.

4.1 Test Set-Up and Procedure

It was determined that the best method to perform the calibration was to place the canard in a fixture resembling the one used in ROBOT-X and then to load the canard at various locations while monitoring the bridge outputs. This canard calibration procedure is hereafter referred to as the CCP. The schematic illustrating the test set up is shown in Figure 8. This was accomplished by using a milling machine as illustrated in Figures 9 to 11.

The loading points were constrained by the available movement of the milling machine bed while the magnitude of the load was limited by the location of the load point. This last limitation was based on the internal geometry of the canard. As noted earlier, pockets are machined out of the canard's ISP casting to reduce weight and rotational inertia, and then the whole casting is covered with fibreglass. If a load point falls in the middle of an air pocket (i.e., between ribs and between the 25% chord line and the trailing edge) the entire load would be supported by the fibreglass skin alone. Considering that the load was to be applied over a 0.25" diameter eraser tipped point (so as to accommodate skin curvature) a practical load limit of 20 lb

was established. This translates to a localized pressure of approximately 400 psi. The exception to this limit was loads applied along the 25% chord line where the skin is immediately backed by ISP. The allowable load limit was increased to 30 lb along this line of action. The resultant load point geometry is shown in Figure 12. The selection of the load points also had the added rationale that in theory:

- a load at point #1 produces an output on the bridge measuring drag but none on the torque or lift bridges,
- the same load at point #4 produces the numerical equivalent of point #1 but on the bridge measuring lift. There will be no output from the bridges measuring drag or torque, and
- the same load applied at point #7 produces an output on the bridge measuring torque, the same lift output as for point #4, and no output of the bridge measuring drag.

4.2 Analysis of the Canard Calibration Procedure

4.2.1 Theoretical Analysis

a) Lift and Drag

$$\epsilon = \frac{\sigma}{E} \quad \text{and} \quad \sigma = \frac{My}{I} \quad \text{or} \quad \epsilon = \frac{My}{EI}$$

where ϵ = strain (in/in)

σ = normal stress (psi)

E = Young's Modulus (10×10^6 psi for aluminum)

M = bending moment (in-lb)

I = area moment of inertia (in^4)

y = distance from the bending neutral axis to the point for which the stress is being calculated.

Substitution of the appropriate values leads to

$$\epsilon_L = \epsilon_D = \frac{4Fd}{E\pi r^3} \qquad (1)$$

where F = applied force

d = moment arm

r = radius of the shaft

y = r (maximum stress at the outermost fibres of the shaft).

b) Torque

$$\epsilon_T = \frac{\tau}{2G} \quad \text{and} \quad \tau = \frac{Tc}{J} \text{ or } \epsilon_T = \frac{Tc}{2GJ} \qquad (2)$$

where τ = shear stress (psi)

G = shear modulus (psi)

J = polar moment of inertia (in^4)

c = distance from the shear neutral axis to the point for which the strain is being calculated.

However from [2], a circular shaft under pure torsion has its principal strain axes rotated 45° from that of the shear strain axis. The gauges pair used to measure the torque on the shaft are tilted at ±45° from the longitudinal axis (see Figure 6) and thus the bridge measures the

principal strains. With the substitution that $G = \frac{E}{2(1+\upsilon)}$ equation (2) reduces to

$$\epsilon_T = \frac{2F\ell(1+\upsilon)}{E\pi r^3} \qquad (3)$$

where c = r (maximum shear at the outer most fibre of the shaft)

ℓ = torque moment arm

F = applied force

υ = Poisson's ratio

Strain is also induced by a shear stress effect [3]. These strains are however cancelled by virtue of the gauge placements (Figure 5) combined with the placement of the active gauges within the wheatstone bridge (Figure 8). For example, for lift [4]:

$$\Delta E_{out} = E_{in} \frac{R_1 R_2}{(R_1+R_2)^2} \left[\frac{\Delta R_1}{R_1} + \frac{\Delta R_{1s}}{R_1} - \frac{\Delta R_2}{R_2} + \frac{\Delta R_{2s}}{R_2} \right] \qquad (4)$$

where E_{in} = voltage applied to the bridge

ΔE_{out} = voltage output of the bridge

R_1 = resistance of gauge #1

ΔR_1 = change in resistance of gauge #1 due to effects other than shear stress

ΔR_{1s} = change in resistance of gauge #1 due to shear effects.

Mechanically, R_1 and R_2 are mounted on opposite sides of the shaft and therefore produce resistance changes of opposite signs. For an upward force, #1 is in compression and therefore $\Delta R_1 < 0$ while #2 is in tension and $\Delta R_2 > 0$. The shear effect, on the other hand, is equivalent to the load divided by the area and is uniformly distributed over the whole section (both ΔR_{1_S} and ΔR_{2_S} are greater than zero). This can be summarized as:

$$\Delta R_1 = -\Delta R_2 \text{ and } \Delta R_{1_S} = \Delta R_{2_S}$$

With the added provision that $R_1 = R_2$ (which is reasonable if the two gauges are from the same lot number), substitution of these values into equation (4) yields

$$\Delta E_{out} = \frac{E_{in}}{2} \left| \frac{\Delta R_1}{R_1} \right| \qquad (5)$$

Examination of equation (5) shows the independence of the bridge outputs from the shear effect. Equations (1) and (3) will be used to determine the theoretical strains of the CCP. Examination of equations (1) and (3) shows that once the relevant strain is known, each equation has a pair of unknowns. These unknowns (F and d or ℓ) can be grouped as an unknown moment or couple so as to make these equations determinate. The implementation of the post flight analysis method will then be used to convert the three moments to meaningful aerodynamic loadings.

4.2.2 Experimental Analysis

The analytically determined strains must undergo an additional correction before comparison to the strains measured during the CCP can take place. This correction must be done to compensate for two factors:

1) the discrepency between the actual gauge factor and the gauge factor set on the portable strain indicator (which was set to give a direct reading of the applied load);

2) the correction for the bridge factor introduced when multiple active arm wheatstone bridges are used.

The two equations of concern are:

$$\epsilon_i K_i = \epsilon_i^* K^* \text{ and } \epsilon_i' = \epsilon_i^* (BF)$$

where ϵ_i = analytically determined strain
ϵ_i^* = strain corrected for gauge factor
ϵ_i' = desired corrected strain
K^* = gauge factor on the portable strain indicator
BF = bridge factor
K_i = gauge factor for strain gauge i

then

$$\epsilon_i' = \frac{\epsilon_i K_i (BF)}{K^*} \qquad (6)$$

For the gauges used on the canards for flight #1:

$$K_L = K_D = 2.15 \qquad K_T = 2.115 \qquad K^* = 1.6$$
$$BF_L = BF_D = 2 \qquad BF_T = 4$$

Table I contains a summary of the analytically expected strains (as derived from equations (1) and (3) and corrected by equation (6)) as a function of load magnitude and load location. Table II contains the experimental results of the CCP.

Comparison of Tables I and II shows the basic accuracy of the theoretical calculations. The minor differences can be attributed to channel crosstalk induced by gauge misalignments.

4.2.3 Calculation of the Crosstalk Matrix, [C]

The crosstalk matrix, [C], is required so as to provide a means to convert the raw measured output of the bridges to a decoupled, analytically relevant set of data. That is

$$\begin{bmatrix} \epsilon'_L \\ \epsilon'_D \\ \epsilon'_T \end{bmatrix} = \begin{bmatrix} C_{11} & C_{12} & C_{13} \\ C_{21} & C_{22} & C_{23} \\ C_{31} & C_{32} & C_{33} \end{bmatrix} \begin{bmatrix} \bar{\epsilon}_L \\ \bar{\epsilon}_D \\ \bar{\epsilon}_T \end{bmatrix}$$

$$\text{or } [\epsilon'] = [C][\bar{\epsilon}] \qquad (7)$$

The data obtained from the CCP is ideally suited for the derivation of [C] since $[\bar{\epsilon}]$ is the measured output (Table II) and $[\epsilon']$ is the analy-

tically corrected strain vector, (Table I). Data obtained from the most extreme locations in combination with the highest load have the highest signal to noise ratio. Therefore, load points 3, 6 and 9 at a load of 20 lb will be used to calculate [C]. It will be shown that only one triplet is required to derive [C].

Load point 3 $[\epsilon'] = \begin{bmatrix} 0 \\ 657 \\ 0 \end{bmatrix}$ and $[\bar{\epsilon}] = \begin{bmatrix} -5 \\ 638 \\ 11 \end{bmatrix}$

Load point 6 $[\epsilon'] = \begin{bmatrix} 657 \\ 0 \\ 0 \end{bmatrix}$ and $[\bar{\epsilon}] = \begin{bmatrix} 633 \\ 43 \\ 10 \end{bmatrix}$

Load point 9 $[\epsilon'] = \begin{bmatrix} 657 \\ 0 \\ -144 \end{bmatrix}$ and $[\bar{\epsilon}] = \begin{bmatrix} 639 \\ 20 \\ -125 \end{bmatrix}$

The determination of the nine elements of the [C] matrix as indicated in equation (7) would require nine independent equations. This is possible since nine load points were used; however, if equation (7) is inverted so as to read

$$[\bar{\epsilon}] = [C]^{-1} [\epsilon'] \qquad (8)$$

this provides a simpler means to determine [C] since equation (8) can then take advantage of the fact that the majority of the theoretically corrected strains are zero.

For example, if equation (8) is expanded for load point 3

$$\begin{bmatrix} -5 \\ 638 \\ 11 \end{bmatrix} = \begin{bmatrix} C_{11} & C_{12} & C_{13} \\ C_{21} & C_{22} & C_{23} \\ C_{31} & C_{32} & C_{33} \end{bmatrix}^{-1} \begin{bmatrix} 0 \\ 657 \\ 0 \end{bmatrix} \qquad (9)$$

it is evident that the elements of the second column of the $[C]^{-1}$ matrix can be uniquely determined. The expansion of equation (8) for load point 6 will similarly allow the determination of the first column of $[C]^{-1}$.

Because the applied torque is coupled to a generated lift moment, the coefficients defined when load point 6 was expanded must be utilized in conjunction with the expansion of load point 9, to derive the third column of the $[C]^{-1}$ matrix. The result is:

$$[C]^{-1} = \begin{bmatrix} 0.963 & -0.008 & -0.044 \\ 0.065 & 0.971 & 0.158 \\ 0.015 & 0.017 & 0.936 \end{bmatrix}$$

$$[C] = \begin{bmatrix} 1.037 & -0.067 & -0.015 \\ 0.008 & 1.032 & -0.019 \\ 0.047 & -0.177 & 1.071 \end{bmatrix}$$

In an ideally decoupled situation the [C] matrix would be an identity matrix. The determined [C] matrix compares favorably in that its major diagonal elements are near to unity while the off-diagonal elements are small. The fact that the off-diagonal elements are not equal to zero indicates the degree of coupling between any given input load (lift, drag, or torque) and the expected strain measurements ($\bar{\epsilon}_L$, $\bar{\epsilon}_D$ and $\bar{\epsilon}_T$).

4.2.4 Performance Checks on [C]

The worst case tested is at the most inboard load points with the lowest load. As a test case, load point 7 (at 10 lb) will be analyzed and the results will be compared to the corrected theoretical strains.

$$[\bar{\epsilon}] = \begin{bmatrix} 157 \\ 5 \\ -65 \end{bmatrix}$$

$$\text{from which } [\epsilon'] = [C][\bar{\epsilon}] = \begin{bmatrix} 160 \\ 6.2 \\ -72.1 \end{bmatrix}$$

This result compares favorably with the results in Table I of

$$[\epsilon'] = \begin{bmatrix} 164 \\ 0 \\ -71.7 \end{bmatrix}$$

Another interesting test is possible if the principle of superposition is used. Consider the following scenario:

- 10 lb applied at load point 3 while
- 20 lb applied at load point 8 and
- 30 lb applied at load point 4.

This results in: a lift moment of 360 in-lb
a drag moment of 120 in-lb
a torque of -40 in-lb

Ideally the measured strains would be the sum of the individual strains from Table II, that is:

$$[\bar{\epsilon}] = \begin{bmatrix} 1 + 479 + 473 \\ 315 + 12 + 33 \\ 6 - 127 + 5 \end{bmatrix} = \begin{bmatrix} 953 \\ 360 \\ -116 \end{bmatrix}$$

Using equation (8) with the determined $[C]^{-1}$ matrix yields:

$$[\bar{\epsilon}] = \begin{bmatrix} 986 \\ 328 \\ -146 \end{bmatrix}$$

Instead of comparing these results to the strains, they will be converted back into moments using the reverse process of equations (6), (3) and (1). This results in a moment vector of:

$$\begin{bmatrix} M_L \\ M_D \\ M_T \end{bmatrix} = \begin{bmatrix} 360.2 \\ 119.8 \\ -40.8 \end{bmatrix}$$

This compares very favorably with the results expected from the principle of superposition.

The determination of the [C] matrix was based on the expansion of loads for one triplet of load points. This in turn requires that the following two questions be answered:

1) Does [C] vary as a function of applied load?
2) Does [C] vary as a function of location?

These two questions can best be answered by examining the effects of applying 10, 20 and 30 lb at each of load points 4, 5 and 6. The comparison will be done by converting the measured strains to their respective moments and then comparing the moment to the actual moment that would be generated by the given load. This comparison will be done by expressing the calculated moment as a percentage of the expected moment. Table III contains the resulting data.

Following are some observations of Table III:

1) The normalized lift varies from 98.0% to 101.1%. This variation does not appear to have a trend when either the load points are kept the same and the load is increased or when the load is kept the same and the application point moves.

2) The normalized drag varies from -0.6% to 2.4%. Again there appears to be no trend either as a function of span or of load.

3) The normalized torque varies from -0.4% to 0.1%. Again there appears to be no trend either as a function of span or of load.

4) The deviation of point 6 with a 20 lb load should be 100% lift, 0% drag and 0% torque since this point was used in generating the [C] matrix. The errors can be attributed to roundoff errors in the calculations.

The conclusion to be reached from the examination of Table III is that since the deviation of the non-loaded axis (in this case drag and torque) varied only from -0.4% to 2.4% maximum and this is well within engineering limits, if any spanwise or load magnitude dependency exists in the canard strain measurements, it can be ignored.

5.0 PREFLIGHT CALIBRATION

For each flight of ROBOT-X it was decided that two preflight checks should be considered. If a new set of instrumented canards was to be installed on the airframe then a canard calibration procedure was to take place. The intent of the procedure was to determine the proper crosstalk coefficient matrix for the canard in question. This procedure is previously outlined in Section 4.0.

The second pre-flight test was to be a shunt calibration of the strain gauge bridges. This procedure would be done on the assembled airframe and would utilize the telemetry subset to be flown with the particular canard. This procedure would provide three pieces of useful information. First of all, it shows that the outputs of the bridges under a simulated load are as expected. Secondly, it demonstrates that the telemetry (signal conditioning plus transmitter/receiver plus the real time processing functions) is operating properly. Thirdly, the calibration points that are required by the telemetry post-processor in the analysis of the flight test data are determined.

5.1 Shunt Calibration

Figure 13 shows a schematic of the in-flight measurement system for the canard strain gauge bridges. As a terminal strip was required

to make the connection between the gauges on the canard and the telemetry system, it was decided that this would be the most convenient location to introduce the shunt calibration resistors. This did, however, require that the lead lengths between the terminal strip and the gauges themselves be considered in the calculation of the shunt resistor value. This is necessary since the resistance in these leads causes an overall desensitization of the bridge. The schematic of shunt calibration is shown in Figure 14. The relationship between the required change in resistance of the gauge due to the introduction of the shunt resistor and the equivalent strain is [5]:

$$\epsilon = \frac{\Delta R}{K R_g}$$

where ϵ = strain to be simulated

R_g = resistance of the strain gauge

ΔR = change in resistance required to simulate the given strain

K = gauge factor.

However K must be rewritten to include the desensitization due to lead resistance:

$$K' = K \frac{R_g}{R_g + R_L}$$

where R_L = lead resistance. Therefore,

$$\epsilon = \frac{\Delta R}{K'R_g} \quad \text{or} \quad \epsilon = \frac{R_g - R_E}{K'R_g} \tag{10}$$

where R_E is the equivalent resistance of the parallel circuit of R_g and R_s. Equation (10) can therefore be rewritten as

$$\epsilon = \frac{R_g - \frac{R_s R_g}{R_s + R_g}}{K'R_g} \tag{11}$$

substituting in the relationship for K' and solving for R_s, yields

$$R_s = \frac{R_g(1-K\epsilon) + R_L}{K\epsilon} \tag{12}$$

Equation (12) is used for determining the shunt calibration resistor for a single active arm wheatstone bridge; however, the bridges used on the canard are multiple active arm and therefore compensation for the bridge factor must be introduced. The result is:

$$R_s = \frac{R_g(1-K\epsilon) + R_L}{K\epsilon\ (BF)} \tag{13}$$

where BF = bridge factor (1 for single active gauge, 2 for two active gauges, 4 for four active gauges).

Since a shunt calibration can only produce a decrease in equivalent resistance, consideration must be given to the relationship

between the shunt calibration and the mechanical aspects of the strain gauge bridges.

The following force sign convention will be used:

1) Positive lift causes a pitch-up of the airframe.
2) Positive drag impedes the forward velocity of the airframe.
3) Positive torque causes pitch-up of the airframe.

With this convention, positive lift would be out of the page in Figure 5 and would therefore cause gauge #1 to be in compression ($\Delta R < 0$) and gauge #2 to be in tension ($\Delta R > 0$). This therefore leads to the conclusion that gauge #1 is to be shunt calibrated for positive lift and gauge #2 is to be shunt calibrated for negative lift. The same logic is applied to the drag and torque bridges.

The determination of the strain value to be used in equation (13) is based upon a combination of material sciences plus the flexibility of the signal conditioning units.

The canard shaft is manufactured from 7075-T6 Aluminum whose rated strain failure is 7500 microstrain and therefore the max/min limits were set to ±7500 microstrain for the first flight. Although it was estimated that the canards were in actuality overdesigned, it was decided that a complete record would be beneficial if failure occurred. It was estimated that these limits would be refined on a flight to flight basis.

Having requested a max/min value for the strain bridges, the designers of the signal conditioning modules then attempted to provide

this value by the selection of appropriate gain control resistors within the signal conditioning modules.

It was decided that the most convenient location to do the shunt calibration was at the Building 15 Test Complex at DRES where the ROBOT-X vehicles are assembled and systems-integrated and which is also the location of the Data Acquisition Center (DAC).

The shunt calibration procedure is as follows:

1) Assemble all the components to be used for a given flight. This includes the appropriate canard, signal conditioning units and telemetry subset.

2) Place the avionics beam where easy access to the signal conditioning is available and make the appropriate connections to the canard strain gauges. In addition a hardwire connection from the telemetry transmitter to the telemetry receiver (in the DAC) is made.

3) Since the telemetred data post-processing software (IDEAS) allows the use of multiple calibration points, up to seven shunt calibration values are determined for each bridge. These calibration points are used to convert the raw data to engineering units.

4) The telemetry subset is powered up and initial bridge balances are done for the strain gauge bridges (zero strain value). Since the telemetry data words are 10 bits wide, each bridge is balanced for a digital count of 512 (one-

half of 2^{10}). This balance is observed in real-time in the DAC.

5) The shunt resistors are then applied and the appropriate change in the bit count is recorded for incorporation into the IDEAS program for post flight analysis.

6) This procedure is repeated for all the strain gauge bridges.

Incorporation of the two calibration procedures is meant to insure that not only is the in-flight instrumentation functioning as designed but also that the data received will be usable in the analysis of the performance of the vehicle.

5.2 Structural Resonance

After the first flight of ROBOT-X in mid-March, 1986, an interesting effect was noted in the response of the canard strain gauge bridges. There appeared to exist a resonance in the output of the drag bridge. A simple measurement of the wave length of the major peaks showed a frequency of approximately 40 Hz. In an effort to ascertain the cause of the resonance, it was decided that a rudimentary structural analysis would take place on the next airframe. This was accomplished by using a Hewlett Packard spectrum analyzer. Since only the frequency was of major concern, the bridges were hooked directly to the analyzer and the canard was excited by striking it a sharp blow with a rubber mallet. After performing a Fast Fourier Analysis the results were as follows:

1) The lift bridge has a natural frequency of approximately 37 Hz.
2) The drag bridge has a natural frequency of approximately 36 Hz.
3) The torque bridge has a natural frequency of approximately 60 Hz.

This resonance appeared to result from a combination of the structural response of the canard with the compliance of the attachment mechanism. It was also noted that any preload in the axis concerned tended to severely limit the amplitude of the oscillation in that axis while slightly increasing the natural frequency and only moderately decreasing the amplitude in the orthogonal axis. Typically the resonant frequency of the orthogonal axis shifted upwards approximately 10 Hz.

Fortunately, a simple solution was available for removing this undesirable measurement characteristic from the data. The original purpose for installing the bridges was to measure the strains produced by aerodynamic forces and the secondary purpose was to attempt to ascertain the frequency response of the canards. To this end, the low pass filters in the signal conditioning modules were tuned to 100 Hz (the estimated frequency response) and as such were not filtering the 40 Hz structural resonance. The answer was simply to retune the low pass filters to 10 Hz. With the 18 dB/octave rolloff of the filters, this meant that the structural resonance would be about 35 dB down at 40 Hz. The validity of this modification was proven in subsequent flights when no undesirable resonances were observed in the strain gauge data.

6.0 REDUCTION OF THE IN-FLIGHT DATA

Having taken reasonable precautions to ensure that the data received from the canards are valid, the method to analyze the data had to be established. The output of the strain gauges can be reduced to only a moment about an appropriate axis (see equations (1) and (3)) and therefore whatever the shape of the canard loading profile, the moments could be resolved as a triad of forces acting at some point on the canard. It is the intent of the analysis to solve for this triad of forces and its application point on the canard.

Figure 15 shows the relationship of the force triad to the global coordinate system. Note that to convert the strain gauge coordinate system to the global coordinate system, two rotations are required. The first is a rotation about the "z" axis through an angle of θ_s which is simply the sweepback angle of the ¼ chord line of the canard relative to the fuselage reference line. The numerical value is derived from the geometry of the canard configuration and is 39°. The second is a rotation about the y' axis through an angle of θ_p (which is the sum of $\gamma + \alpha_c$). In an idealized situation the unknown force triplet acts at an application point (AP) which is defined as the intercept of the ¼ chord line of the canard with a line drawn perpendicular to the ¼ chord line which passes through the area centroid of the canard planform (see Figure 16). If the distance from the centre of the strain gauge group to the AP is called "A", then in the ideal case, the coordinates of AP in the x'y'z' system are:

$$AP = (0, -A, 0)$$

Since the canards are non-ideal the above equation requires that deviations be introduced in defining the location of the AP. Therefore, let the coordinates of AP be given by:

$$AP = (\xi_1, -A - \xi_2, \xi_3)$$

where ξ_1, ξ_2 and ξ_3 are deviations due to manufacturing and aerodynamic effects.

Based upon the BOC drawings and physical locations of the strain gauges,

$$A = 9.928".$$

If R_1, R_2 and R_3 are the magnitudes of the force triplet in the xyz coordinate system, then it can be shown that a rotation about "z" through "θ_s" and then a rotation about "y'" through "θ_p" yields

$$\begin{bmatrix} R_1' \\ R_2' \\ R_3' \end{bmatrix} = \begin{bmatrix} \cos\theta_p\cos\theta_s & \cos\theta_p\sin\theta_s & -\sin\theta_p \\ -\sin\theta_s & \cos\theta_s & 0 \\ \sin\theta_p\cos\theta_s & \sin\theta_p\sin\theta_s & \cos\theta_p \end{bmatrix} \begin{bmatrix} R_1 \\ R_2 \\ R_3 \end{bmatrix} \qquad (14)$$

where R_1', R_2' and R_3' are the magnitudes of the force triplet in the x'y'z' coordinate system.

Equation (14) is the desired result since it provides the triaxial components of the unknown force triad in the strain gauge coordinate system.

Measuring the distances to the CP in the x'y'z' coordinates yields

$$\begin{bmatrix} d_{x'} \\ d_{y'} \\ d_{z'} \end{bmatrix} = \begin{bmatrix} \xi_1 \\ -(A+\xi_2) \\ \xi_3 \end{bmatrix} \tag{15}$$

Note that the application point AP is assumed to rotate about the y' axis while the force triplet is assumed to remain in the global coordinate system.

The strain gauge bridges are configured to measure the resultant moments and therefore the moments generated by [F] must be found. This process is the simple summation of moments. Using the sign convention of Section 5.1,

$$M_{x'} = -(d_{y'}) R_3' + (d_{z'}) R_2' \tag{16}$$

$$M_{y'} = -(d_{x'}) R_3' + (d_{z'}) R_1' \tag{17}$$

$$M_{z'} = (d_{x'}) R_2' - (d_{y'}) R_1' \tag{18}$$

The force components required to determine equations (16), (17) and (18) are found in equation (14) while the displacement components are found in equation (15). An examination of these equations shows that there will be six unknowns: R_1, R_2, R_3, ξ_1, ξ_2 and ξ_3; however,

there are only three equations. To make this a determinate system the following assumptions are made:

1) $R_2 = 0$ This states that the side force F_y is zero which is valid under typical flight conditions, i.e., angle of sideslip is approximately zero.

2) $\xi_2 = 0$ This states that the load point AP does not vary along the "y'" axis which is also valid under typical flight conditions.

3) $\xi_3 = 0$ This states that the AP deviation in the "z'" axis is zero which is a reasonable assumption due to the easily manufactured, thin, symmetric cross-section of the canard.

Accepting these assumptions, substituting the required values from equations (14) and (15) into equations (16), (17) and (18) and then reducing yields

$$\begin{bmatrix} M_{x'} \\ M_{y'} \\ M_{z'} \end{bmatrix} = \begin{bmatrix} 0 & R_1\sin\theta_p + R_3\cos\theta_p & -R_1\sin\theta_s \\ -R_1\sin\theta_p\cos\theta_s - R_3\cos\theta_p & 0 & R_1\cos\theta_p\cos\theta_s - R_3\sin\theta_p \\ -R_1\sin\theta_s & R_1\cos\theta_p\cos\theta_s - R_3\sin\theta_p & 0 \end{bmatrix} \begin{bmatrix} \xi_1 \\ A \\ 0 \end{bmatrix} \quad (19)$$

Making the substitutions:

$$K_1 = \sin\theta_p\cos\theta_s$$
$$K_2 = \cos\theta_p$$
$$K_3 = \sin\theta_s$$

$$K_4 = \cos\theta_p \cos\theta_s$$
$$K_5 = \sin\theta_p$$

into equation (19) and rewriting yields:

$$M_{x'} = A(R_1K_1 + R_3K_2)$$
$$M_{y'} = -\xi_1(R_1K_1 + R_3K_2)$$
$$M_{z'} = -\epsilon_1K_3 + A(R_1K_4 - R_3K_5)$$

Solving these three equations simultaneously yields:

$$\xi_1 = \frac{-M_{y'}A}{M_{x'}} \tag{20}$$

$$R_1 = \frac{M_{z'} - \dfrac{AM_{y'}K_3}{M_{x'}} + \dfrac{K_5M_{x'}}{K_2}}{A\left(\dfrac{K_5K_1}{K_2} + K_4\right)} \tag{21}$$

$$R_3 = \frac{M_{x'}}{K_2A} - \frac{R_1K_1}{K_2} \tag{22}$$

Note that equation (22) requires that equation (21) be solved first.

As an illustration of the procedures involved, a sample calculation will be performed.

7.0 A POST FLIGHT ANALYSIS NUMERICAL EXAMPLE

As an illustration of the procedure to be used in the reduction of the flight test data, Figures 17 through 21 show the data traces from the first few seconds of flight #2 which took place in late July 1986. The launch took place at approximately 52.2 seconds on the time scale in the Figures. These graphs were produced by the IDEAS post-processor and the appropriate calibration constants were used to convert the ordinate of each graph into engineering units. As an arbitrary example, consider the time T = 54 sec. At this point:

$$\bar{\epsilon}_L = 1575\ \mu\epsilon \qquad \bar{\epsilon}_D = 48\ \mu\epsilon \qquad \bar{\epsilon}_T = -16\ \mu\epsilon$$
$$\gamma = 5.2° \qquad \alpha_c = 6.5°$$

As this was the second instrumented canard, a pre-flight CCP was performed and the resultant crosstalk matrix determined.

$$[\epsilon] = \begin{bmatrix} 1.014 & 0.063 & -0.053 \\ -0.080 & 1.035 & -0.054 \\ 0.003 & -0.154 & 1.040 \end{bmatrix} \begin{bmatrix} 1575 \\ 48 \\ -16 \end{bmatrix}$$

$$\text{from which } [\epsilon] = \begin{bmatrix} 1593 \\ 152 \\ -102.2 \end{bmatrix}$$

Using equations (1) and (3) to derive the moments yields

$$M_L = 1564 = M_{x'},$$
$$M_D = 149 = M_{z'},$$
$$M_T = -150.9 = M_{y'},$$

Substituting $\theta_s = 39°$, $\theta_p = \alpha_c + \gamma = 6.5 + 5.2 = 11.7°$, and the above derived moments into equations (19) through (22) yields

$$\xi_1 = 0.958"$$
$$R_1 = 60.1 \text{ lb}$$
$$R_3 = 151.2 \text{ lb}$$

This result is illustrated in Figure 22. At that instant in time (T = 54 secs) with the given angle of attack of the canard, these derived values will produce the strains as measured by the strain gauge bridges.

The purpose of this example is to simply illustrate the procedure used to derive useful aerodynamic data. A detailed analysis to ascertain the significance of these numbers will be the subject of a subsequent report which will be issued when the analysis of data from a number of flights has been completed.

8.0 CONCLUDING REMARKS

The intent of this report has been to illustrate the means to measure the aerodynamic forces on the ROBOT-X canards. This was accomplished by designing a transducer circuit composed of three strain gauge bridges. As for any transducer, a means to calibrate and verify

the output of these strain gauge bridges was developed. To date, the general trends of the strain data correlate well with what can be inferred from the other on-board transducers, the autopilot responses, and the performance of the vehicle.

REFERENCES

[1] Beckwith and Buck, "Mechanical Measurements", 2nd Edition, Addison-Wesley Publishing Co., 1973, pp 326-335.

[2] Popov, E.P., "Mechanics of Solids", 2nd Edition, Prentice Hall Inc., 1976, pp 258-263.

[3] Popov, E.P., "Mechanics of Solids", 2nd Edition, Prentice Hall Inc., 1976, pp 174-183.

[4] Murray, W.M. and Stein, P.K., "Strain Gauge Techniques", Academic Press, 1963, Chapter XII.

[5] Anonymous, "Temperature Induced Apparent Strain and Gauge Factor Variations in Strain Gauges", Micromeasurements Group Inc., 1976, Technical Bulletin No. TN504, pg. 8.

[6] Anonymous, Basic of Strain Gauge Instrumentation", Pacific Instruments Inc., Application Note, pg. 103.

Load Point Number (see Fig. 12)	Load = 10 lb			Load = 20 lb			Load = 30 lb		
	Lift ϵ'_L	Drag ϵ'_D	Torque ϵ'_T	Lift ϵ'_L	Drag ϵ'_D	Torque ϵ'_T	Lift ϵ'_L	Drag ϵ'_D	Torque ϵ'_T
1	0	164	0	0	328	0	-	-	-
2	0	246	0	0	493	0	-	-	-
3	0	328	0	0	657	0	-	-	-
4	164	0	0	328	0	0	493	0	0
5	246	0	0	493	0	0	739	0	0
6	328	0	0	657	0	0	985	0	0
7	164	0	-71.7	328	0	-144	-	-	-
8	246	0	-71.7	493	0	-144	-	-	-
9	328	0	-71.7	657	0	-144	-	-	-
10	164	0	-144	328	0	-288	-	-	-
11	246	0	-144	493	0	-288	-	-	-
12	328	0	-144	657	0	-288	-	-	-

Units are microstrain.

TABLE I CORRECTED THEORETICAL STRAINS

Load Point Number (see Fig. 12)	Load = 10 lb			Load = 20 lb			Load = 30 lb		
	Lift $\bar{\epsilon}_L$	Drag $\bar{\epsilon}_D$	Torque $\bar{\epsilon}_T$	Lift $\bar{\epsilon}_L$	Drag $\bar{\epsilon}_D$	Torque $\bar{\epsilon}_T$	Lift $\bar{\epsilon}_L$	Drag $\bar{\epsilon}_D$	Torque $\bar{\epsilon}_T$
1	-3	154	2	-7	314	4	-	-	-
2	2	239	6	4	476	11	-	-	-
3	1	315	6	-5	638	11	-	-	-
4	155	12	2	318	29	4	473	33	5
5	236	16	4	473	33	7	713	45	10
6	317	21	5	633	43	10	960	57	5
7	157	5	-65	318	10	-128	-	-	-
8	236	6	-63	479	12	-127	-	-	-
9	317	8	-63	639	20	-125	-	-	-
10	165	0	-132	330	2	-263	-	-	-
11	243	11	-128	492	18	-259	-	-	-
12	325	19	-128	653	35	-257	-	-	-

TABLE II EXPERIMENTAL RESULTS OF THE CCP

	Load = 10 lb				Load = 20 lb				Load = 30 lb			
	Lift	Drag	Torque	L_A	Lift	Drag	Torque	L_A	Lift	Drag	Torque	L_A
4	58.8 (98.0)*	0.6 (1.0)	-0.1 (-0.2)	60	120.6 (100.5)	2.9 (2.4)	-0.3 (-0.3)	120	179.4 (99.7)	0.5 (0.3)	-0.7 (-0.4)	180
5	89.5 (99.4)	0.01 (0.01)	0.1 (0.1)	90	179.4 (99.7)	0.4 (0.2)	-0.1 (-0.1)	180	270.4 (100.1)	-1.1 (-0.4)	-0.3 (-0.1)	270
6	120.3 (100.3)	-0.1 (-0.1)	0.03 (0.03)	120	240.1 (100.0)	0.1 (0.04)	0.03 (0.01)	240	364.0 (101.1)	-2.3 (-0.6)	-2.9 (-0.8)	360

L_A is the actual value of the lift moment generated, which is used in normalizing the measured moments.

* Normalized value calculated by $1/L_A$ times measured moment (percent).

TABLE III SENSITIVITY CHECK OF [C] MATRIX

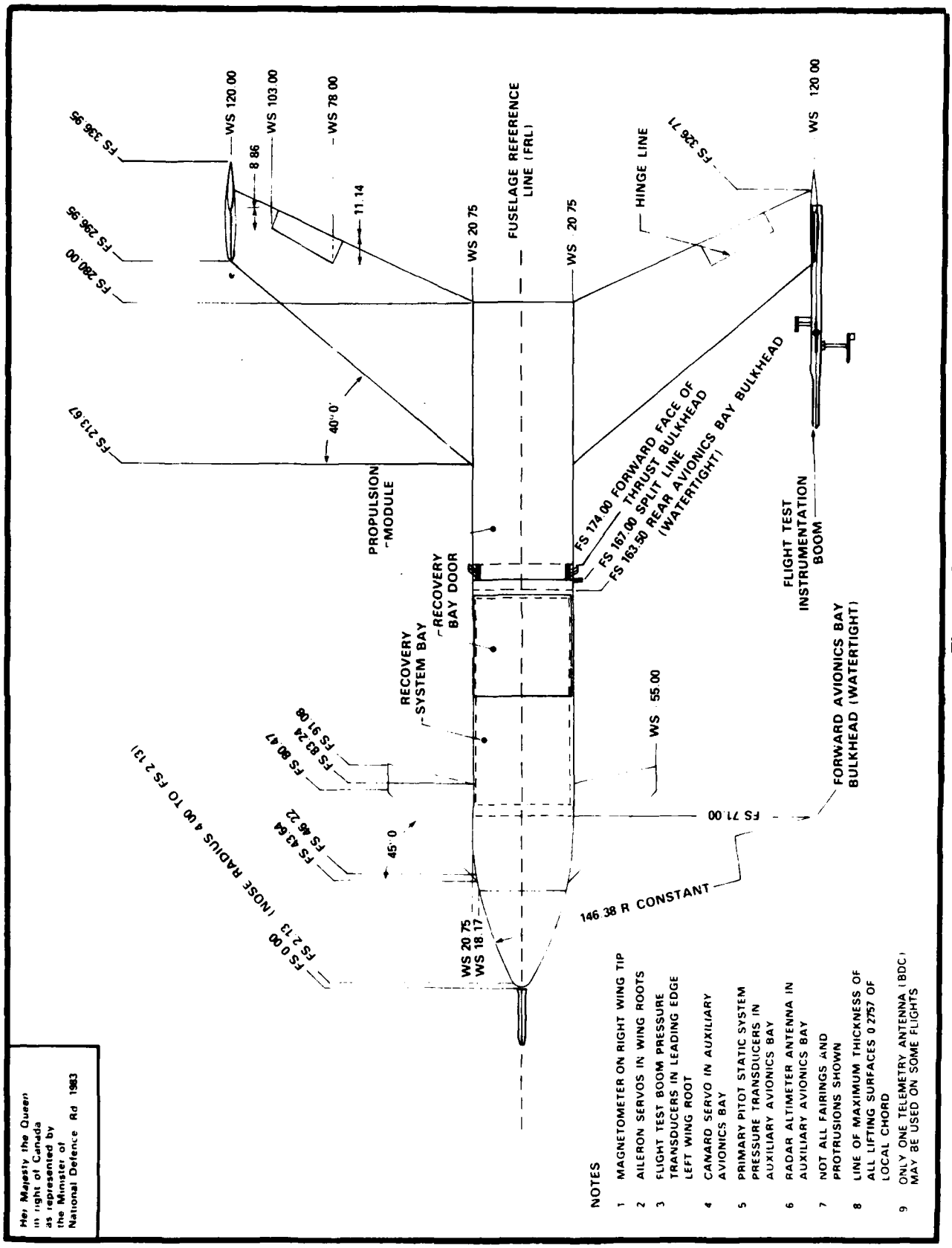

Figure 1

ROBOT – X CONFIGURATION
(Top View Looking Down)

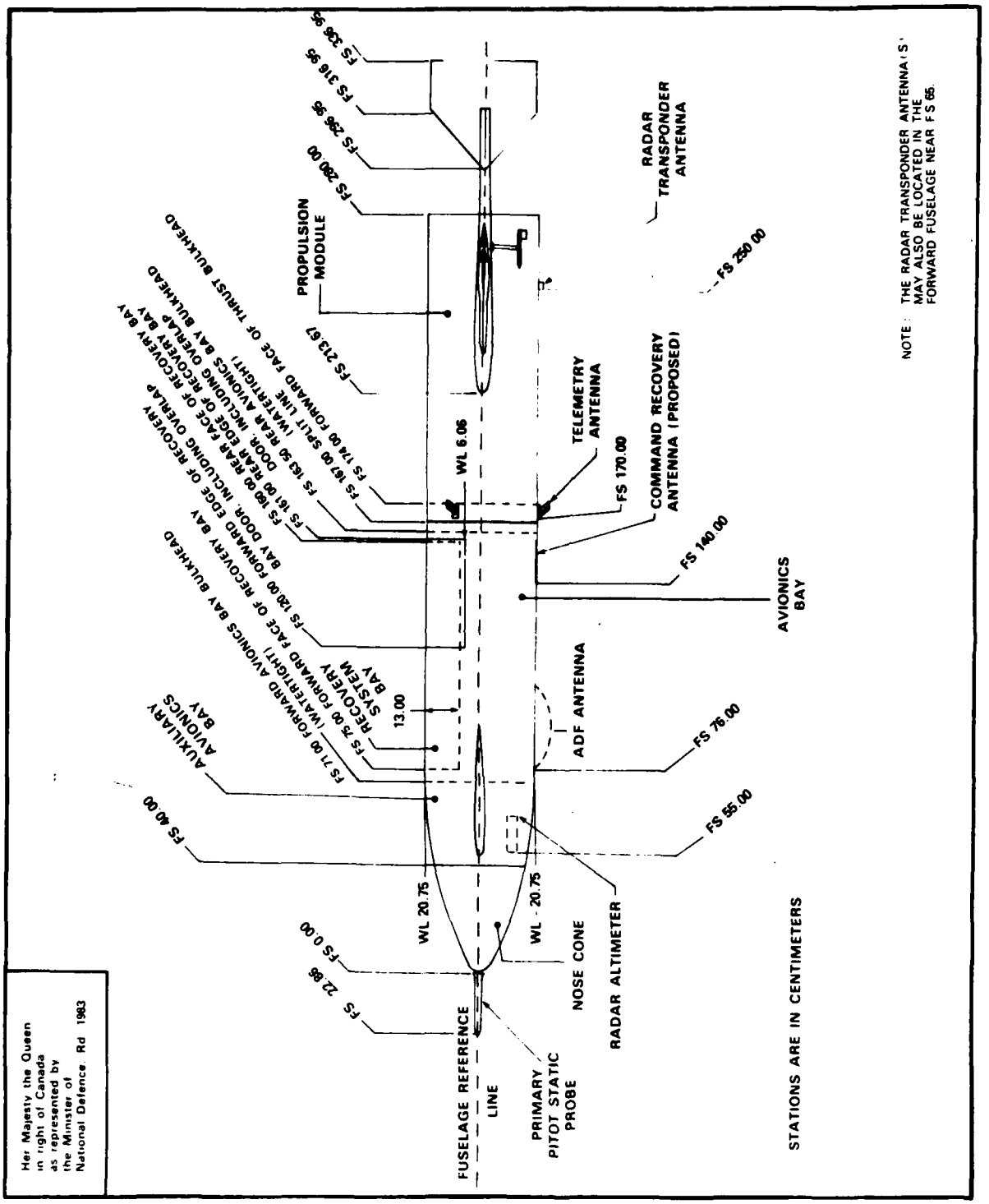

Figure 2

ROBOT – X CONFIGURATION

(Side View)

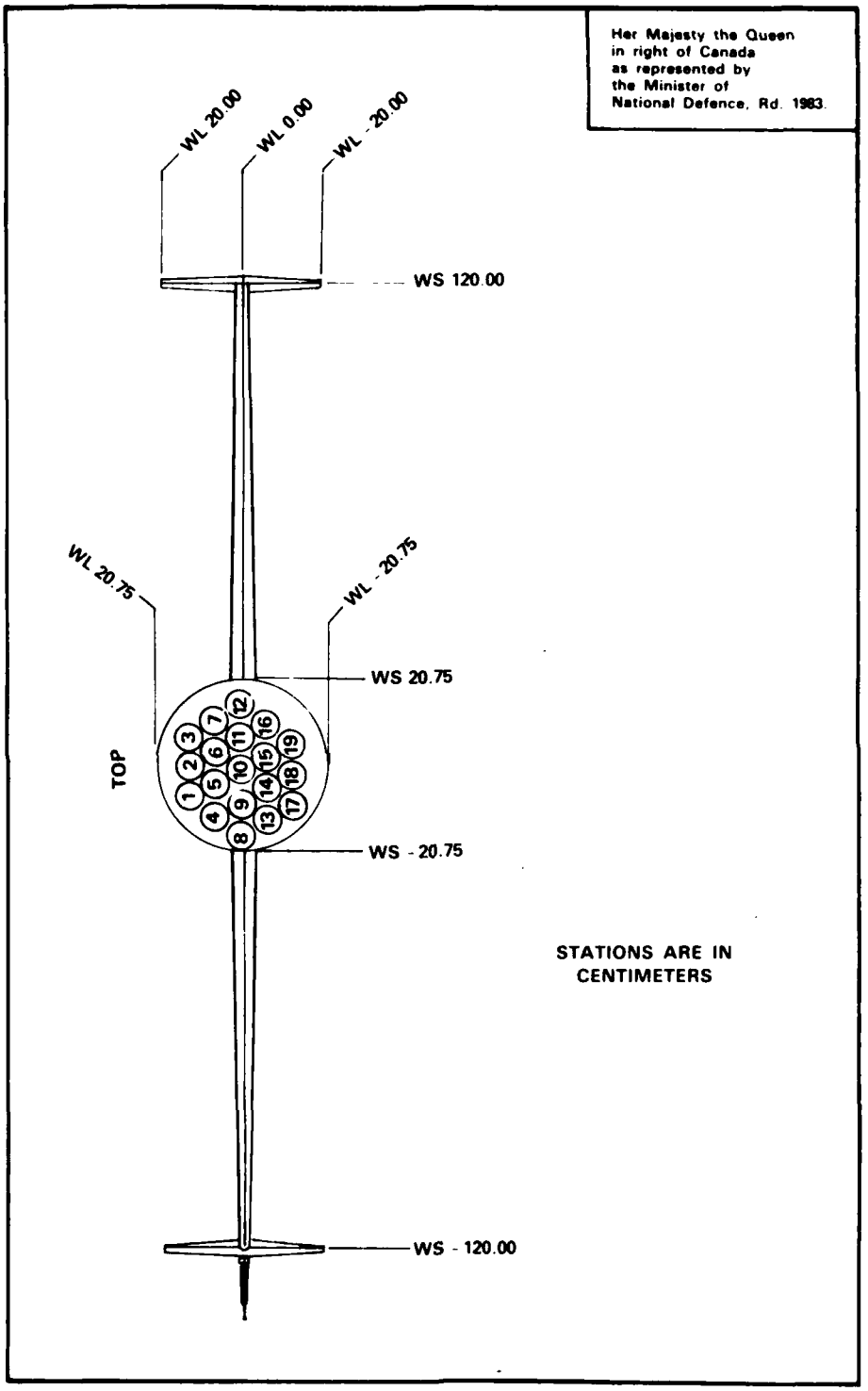

Figure 3

ROBOT – X CONFIGURATION
(Aft View Looking Forward)

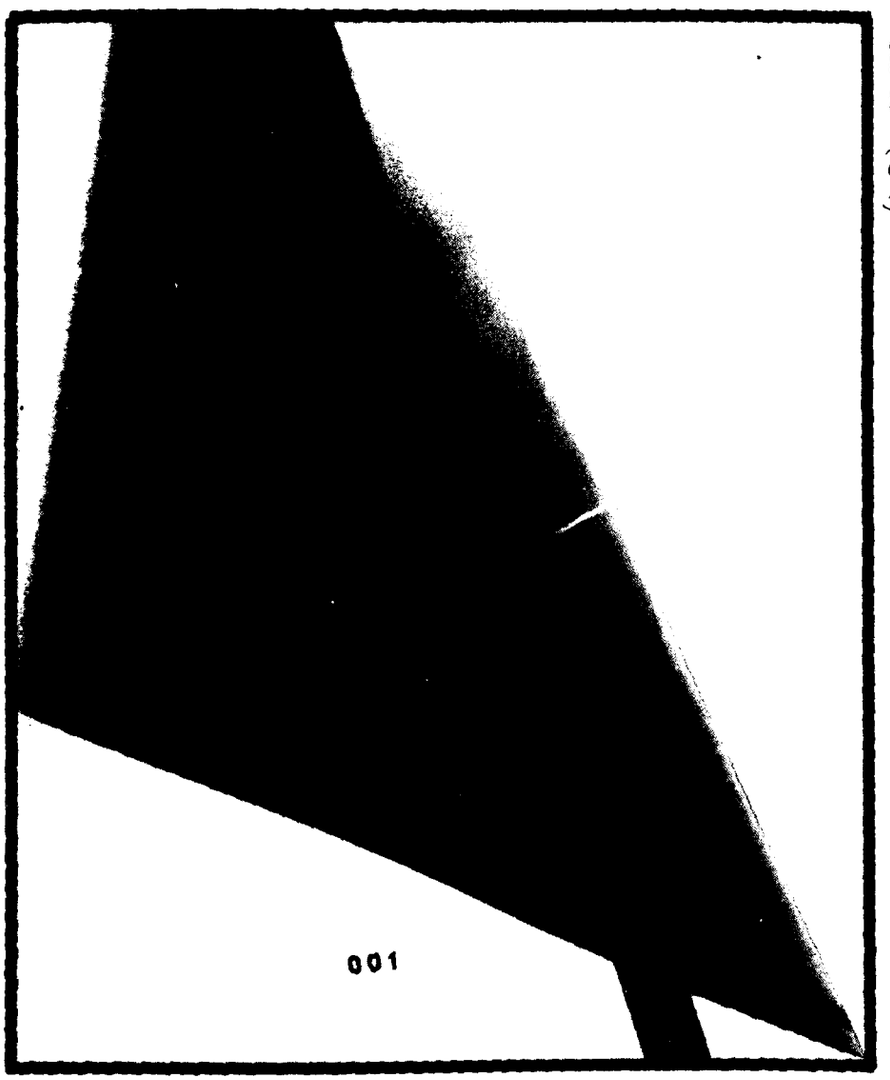

Figure 4

INTERNAL STRUCTURE OF THE CANARDS

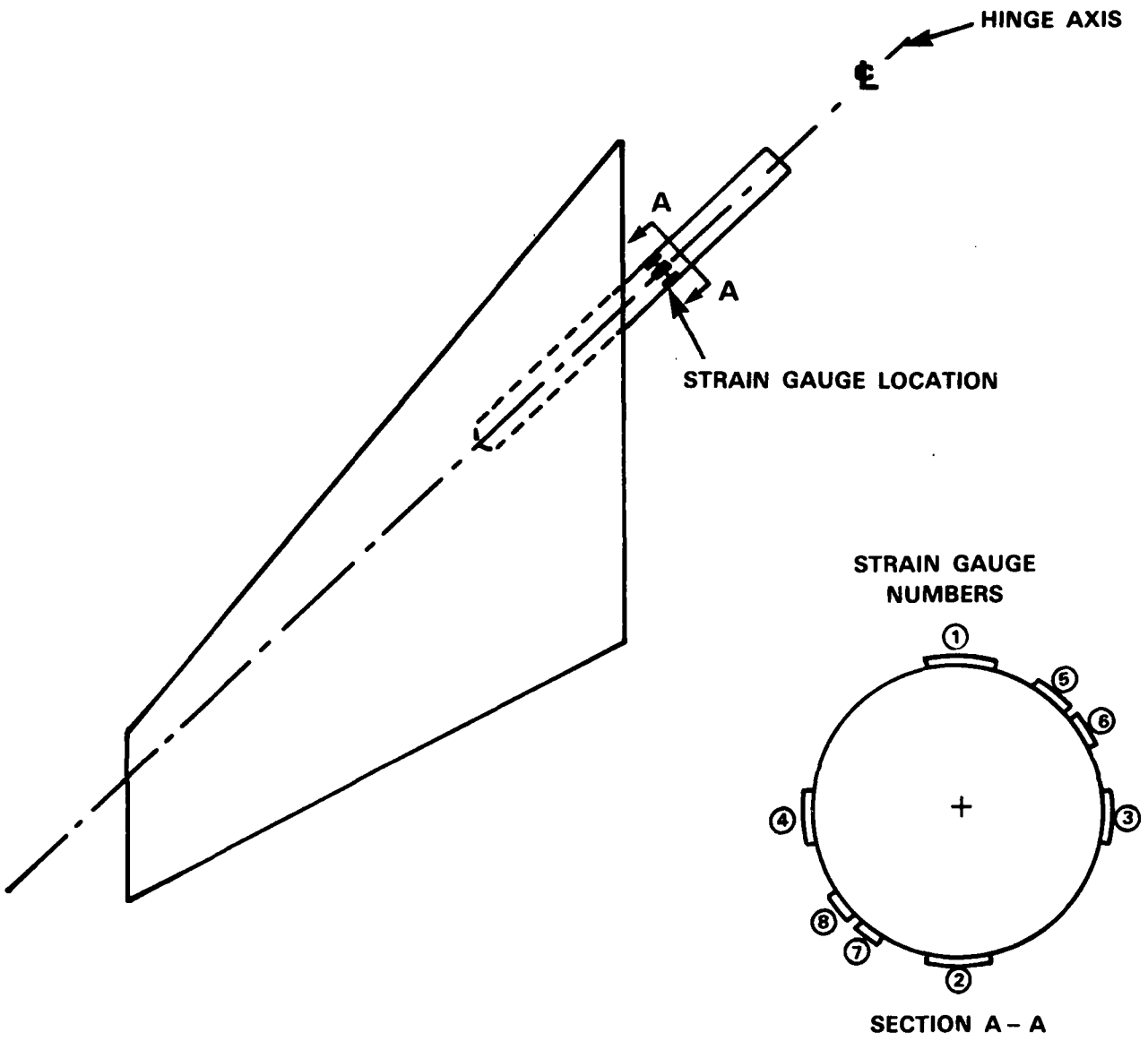

Figure 5

LOCATION OF STRAIN GAUGES

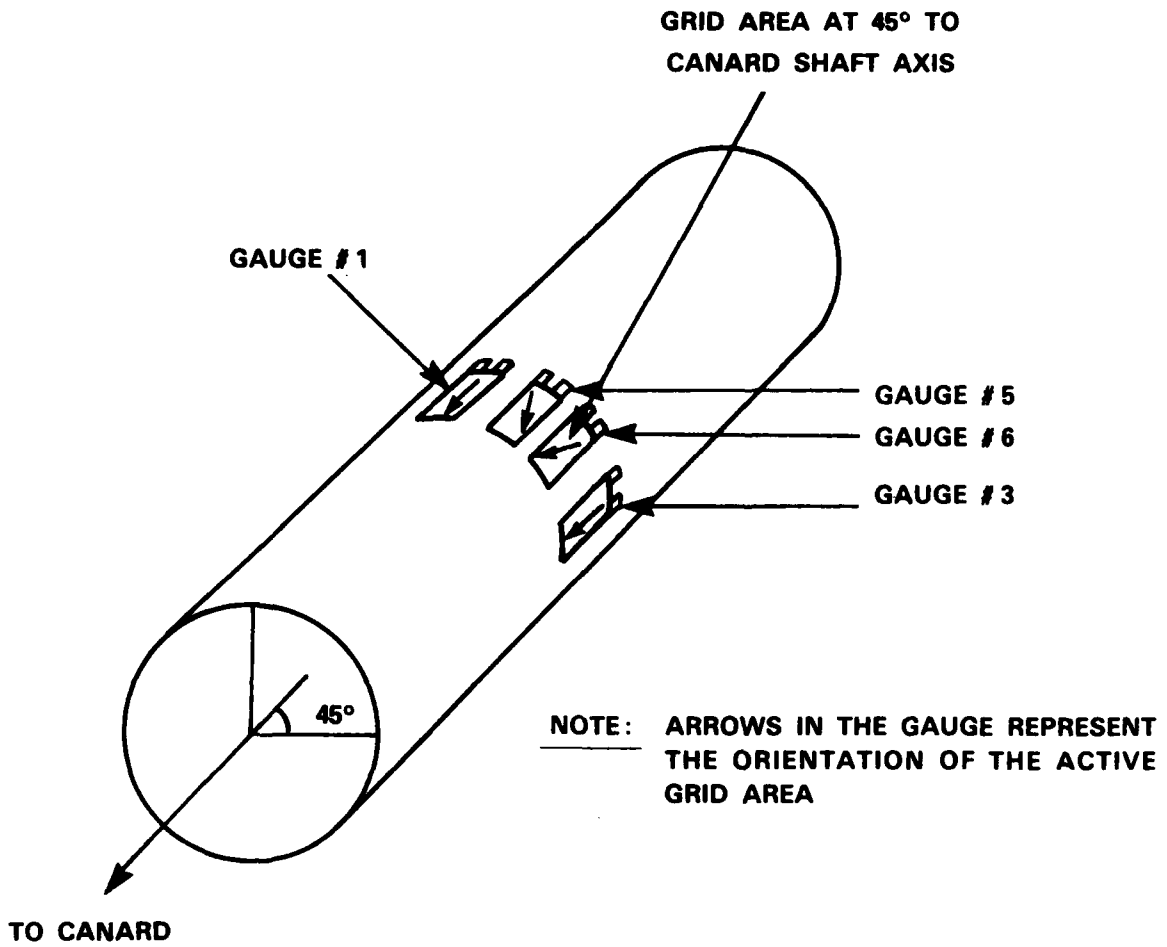

Figure 6

GAUGE ORIENTATIONS ON THE CANARD SHAFT

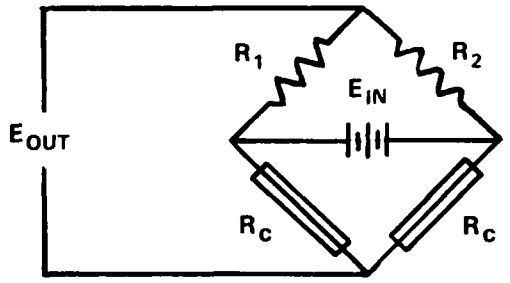

NOTE:

R_C – COMPLETION RESISTOR

R_* – STRAIN GAUGE NO. *

BRIDGE FACTOR = 2

LIFT MEASUREMENT

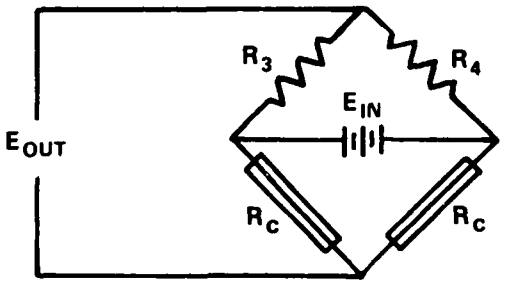

BRIDGE FACTOR = 2

DRAG MEASUREMENT

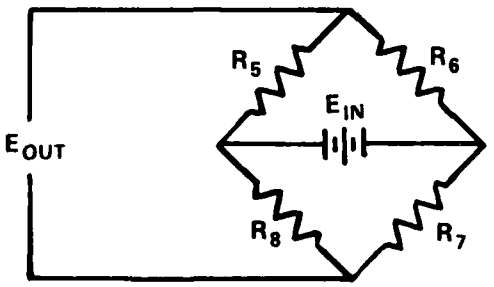

BRIDGE FACTOR = 4

TORQUE MEASUREMENT

Figure 7

WHEATSTONE BRIDGE CIRCUITS

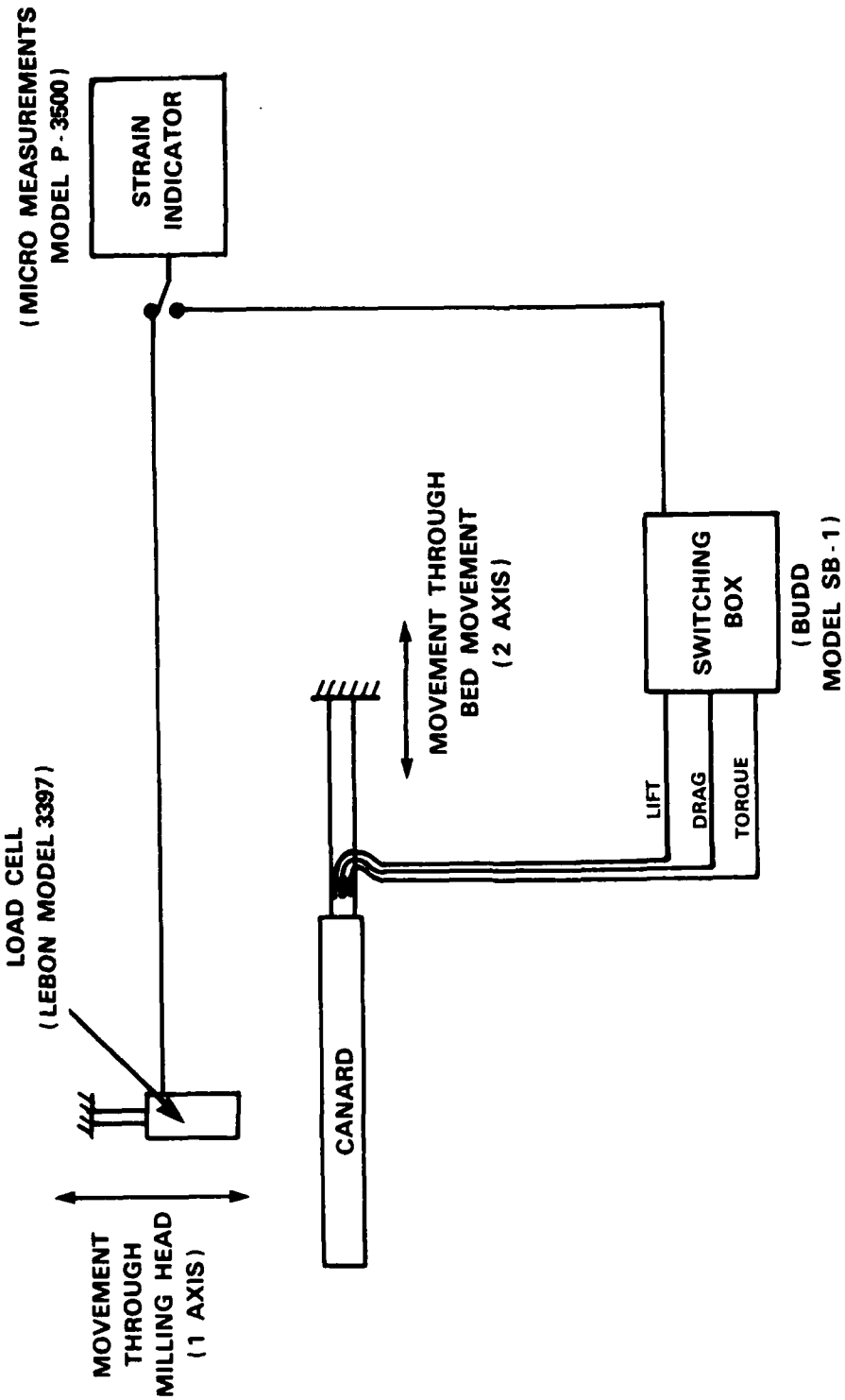

Figure 8

CCP TEST SCHEMATIC

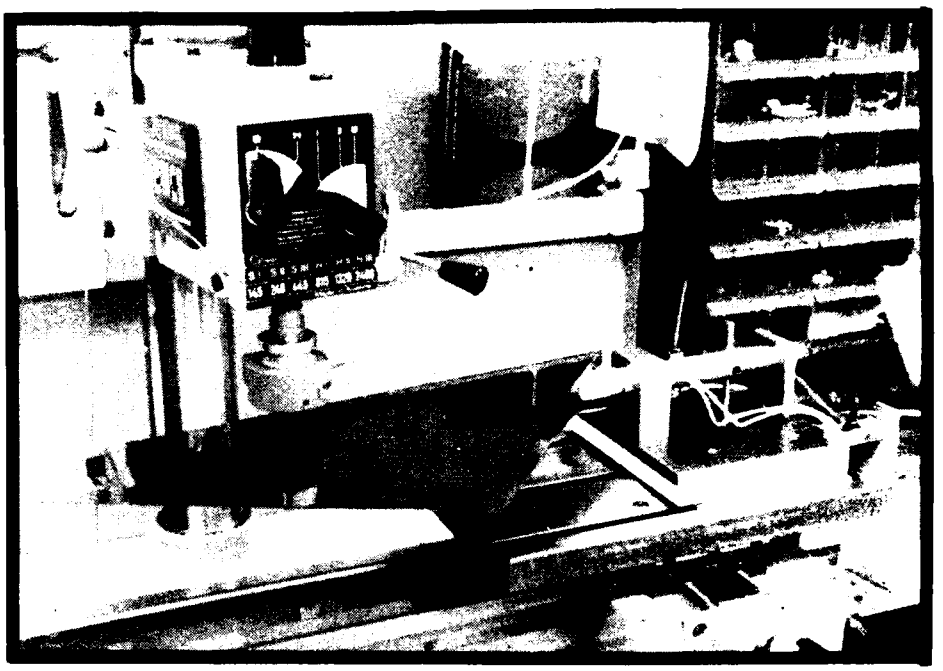

Figure 9

CCP TEST SET UP

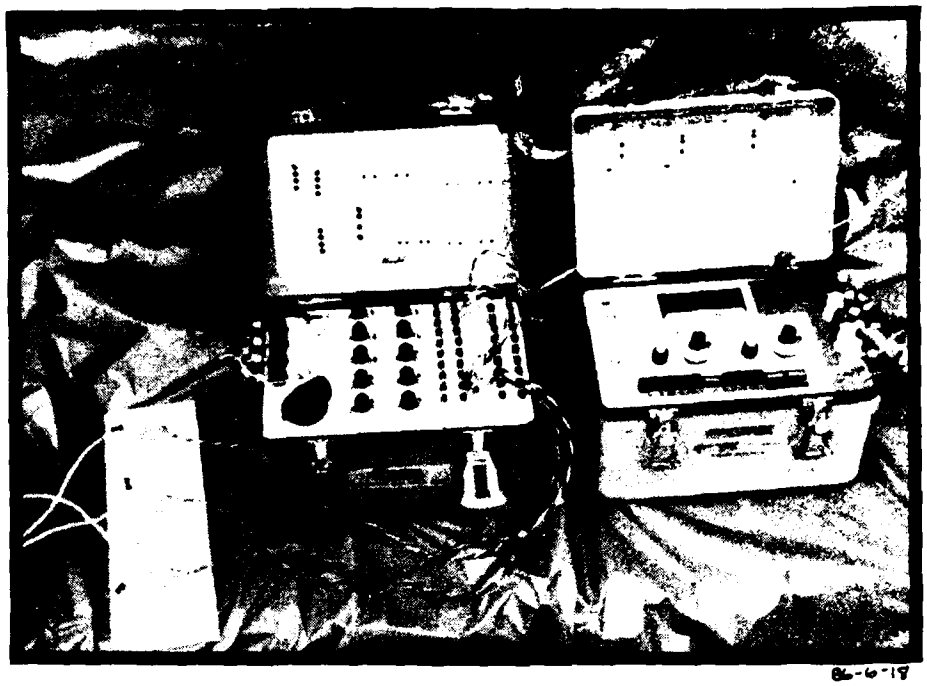

Figure 10

OVERVIEW OF THE CCP TEST INSTRUMENTATION

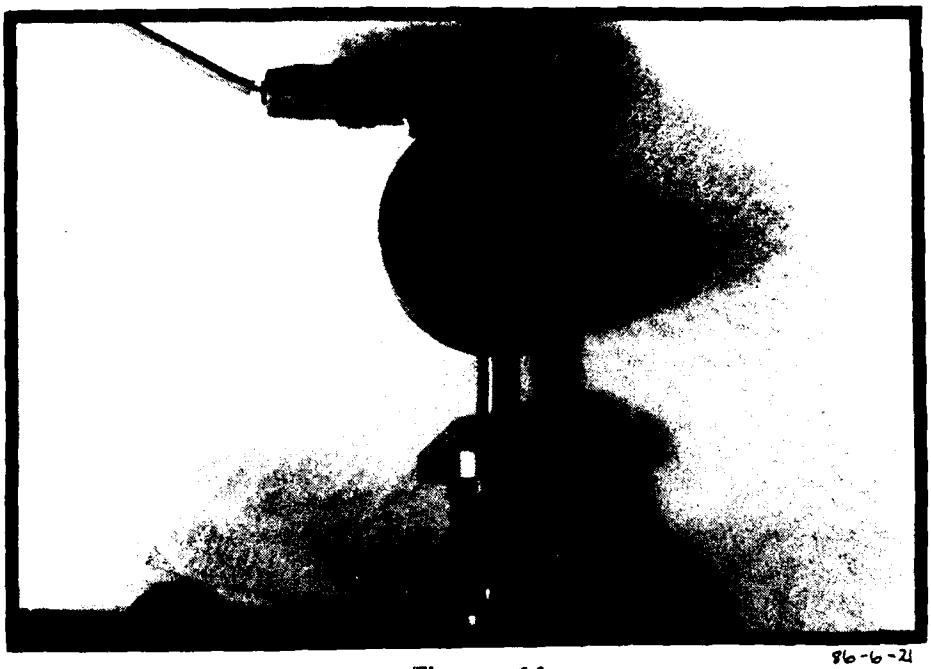

Figure 11

LOAD CELL USED DURING THE CCP

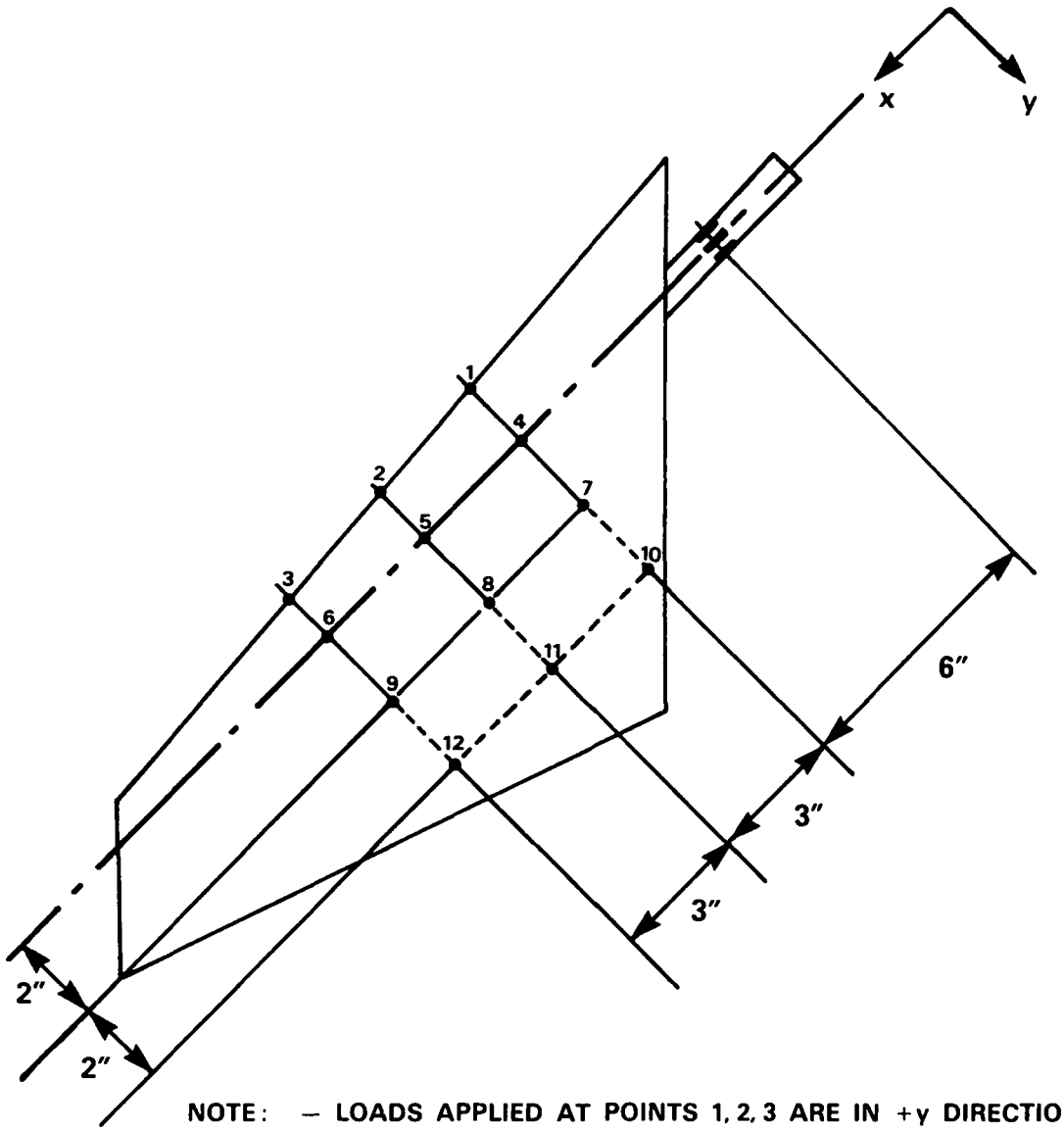

NOTE: – LOADS APPLIED AT POINTS 1, 2, 3 ARE IN +y DIRECTION
– LOADS AT POINTS 4 – 9 ARE IN –z DIRECTION
– LOAD POINTS 10 – 12 ARE ON THE OPPOSITE SURFACE OF THE CANARD FROM LOAD POINTS 4 – 9 AND THE LOADS ARE APPLIED IN THE +z DIRECTION

Figure 12

LOAD POINT CONFIGURATION

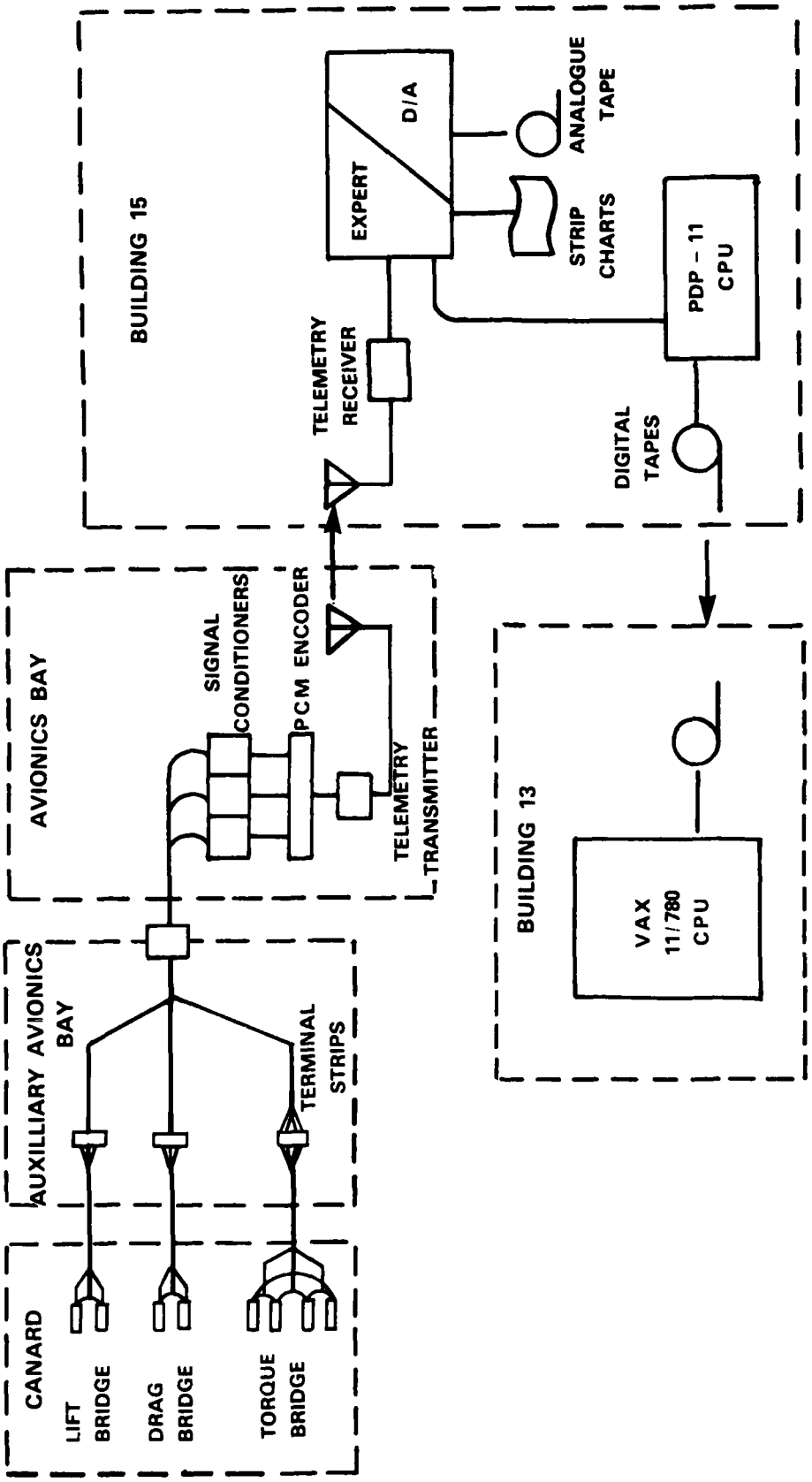

Figure 13

SCHEMATIC OF THE IN – FLIGHT MEASUREMENT SYSTEM

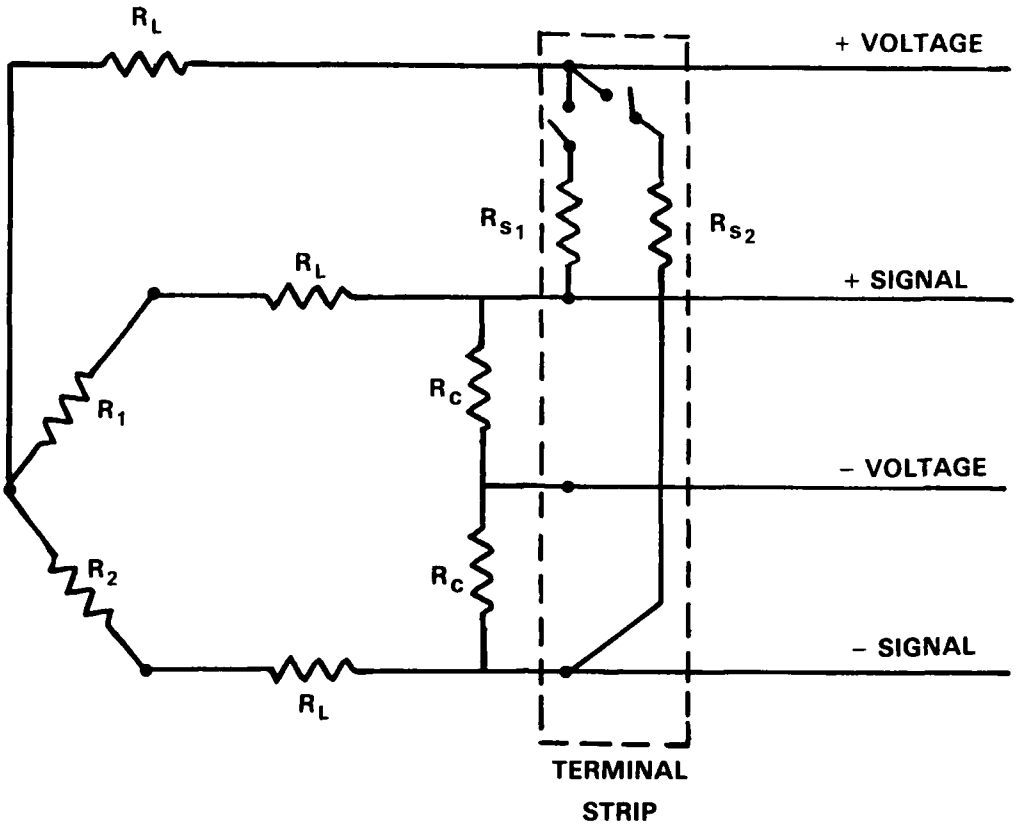

Figure 14

SHUNT CALIBRATION CIRCUIT

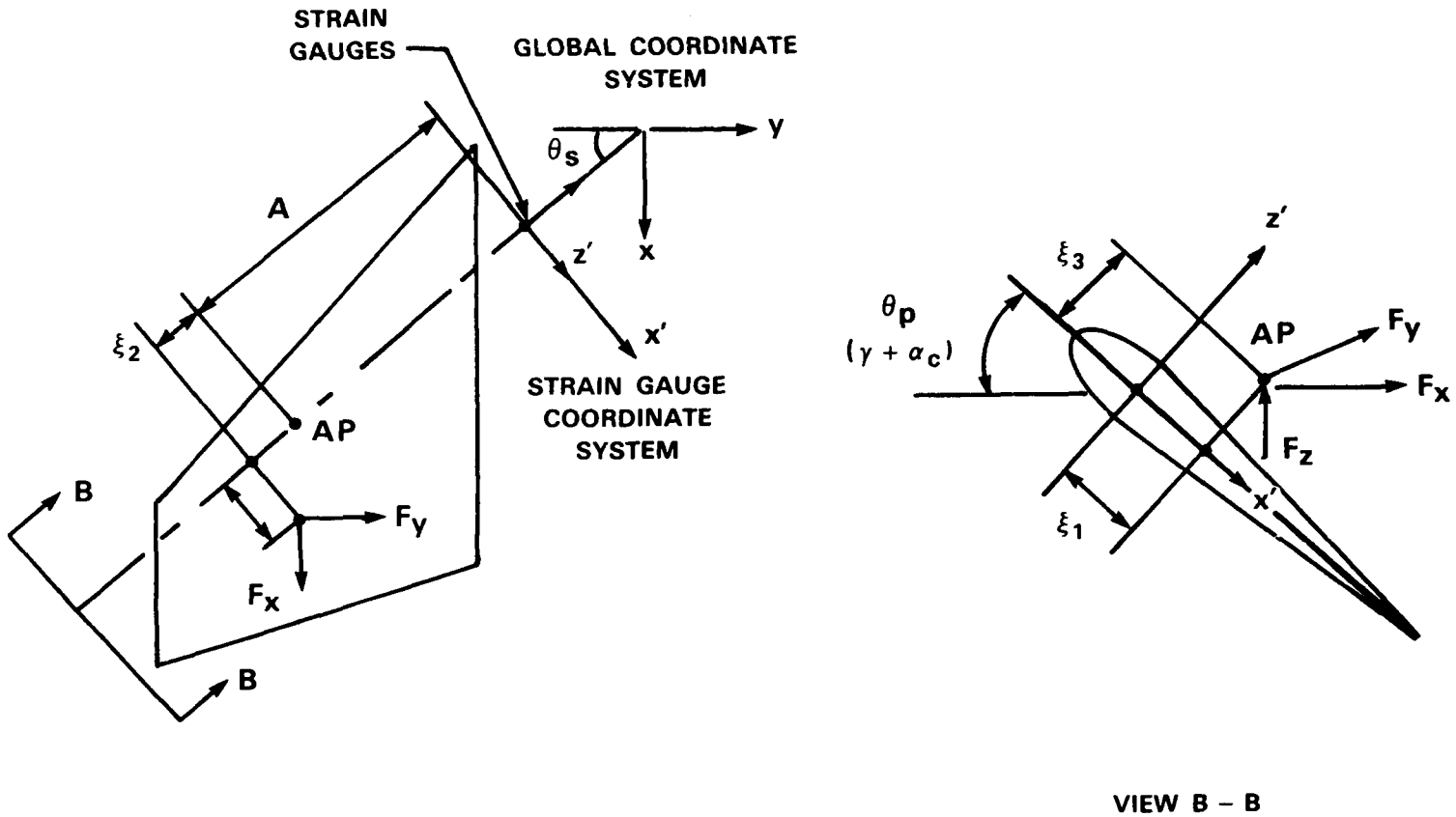

Figure 15

FORCE COORDINATE SYSTEM FOR THE CANARDS

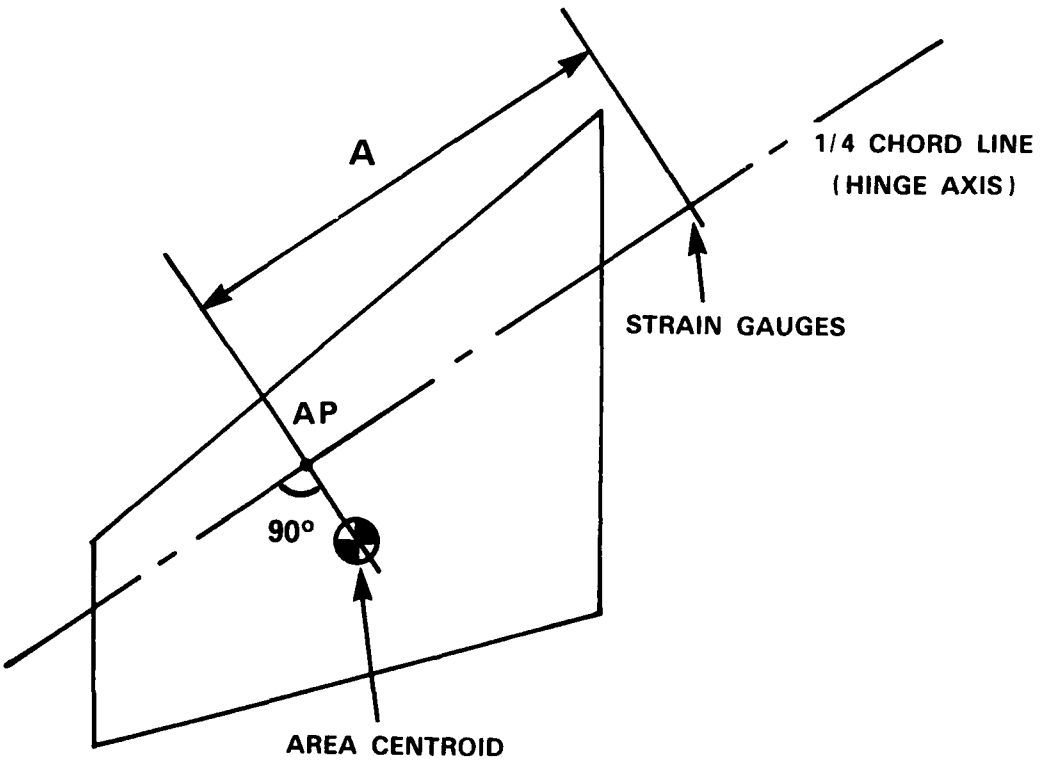

Figure 16

THE DETERMINATION OF THE CONSTANT "A"

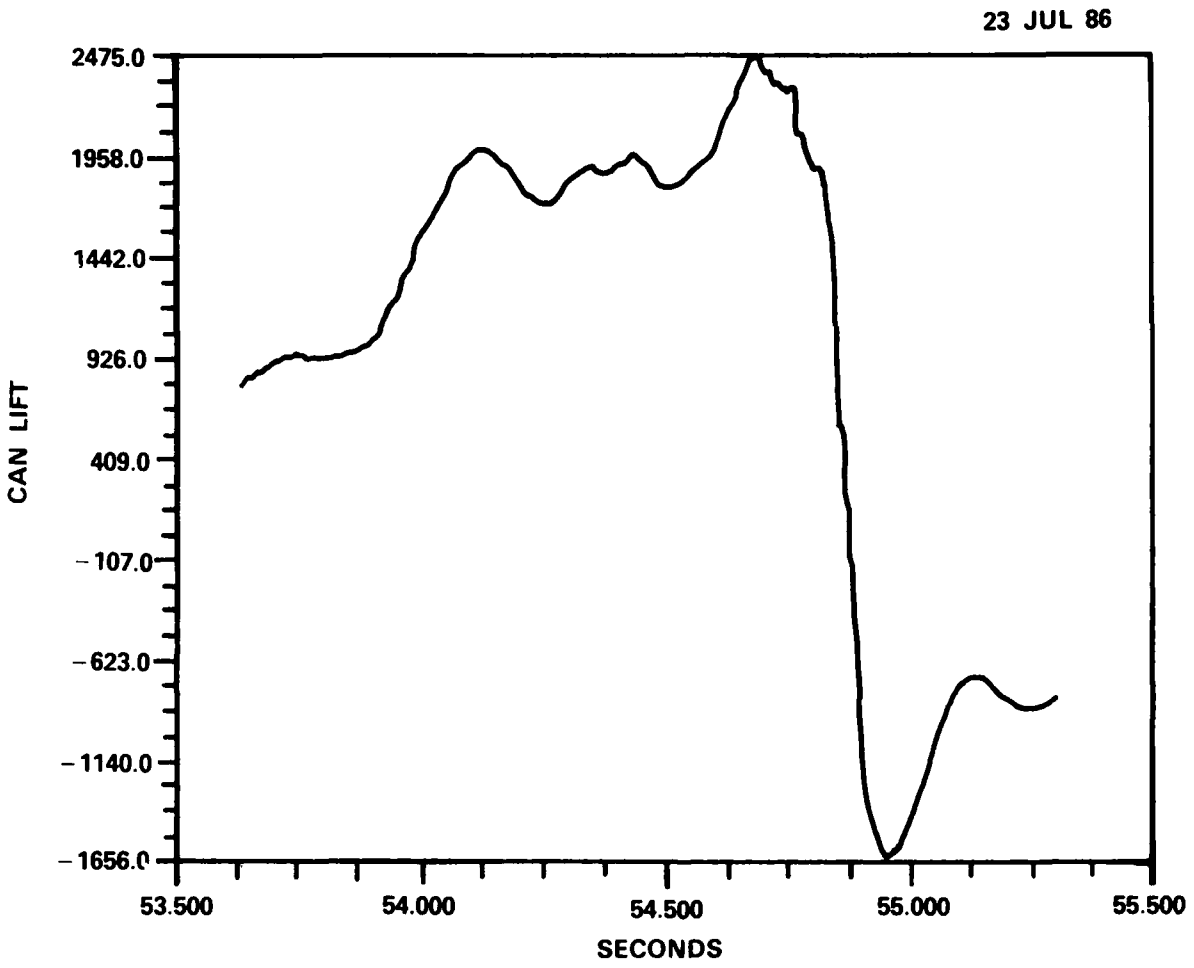

Figure 17

TRACE OF LIFT FOR FLIGHT # 2

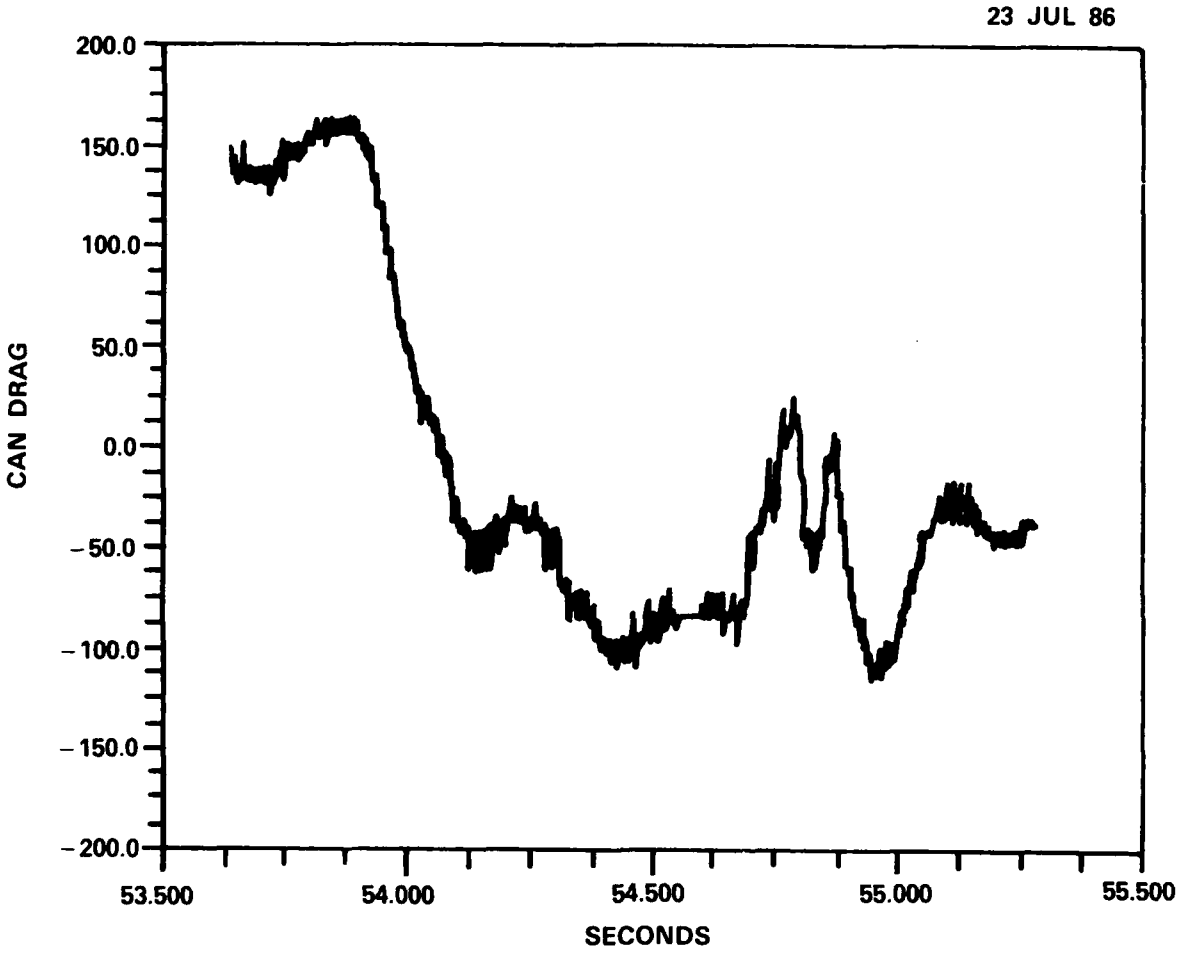

Figure 18

TRACE OF DRAG FOR FLIGHT # 2

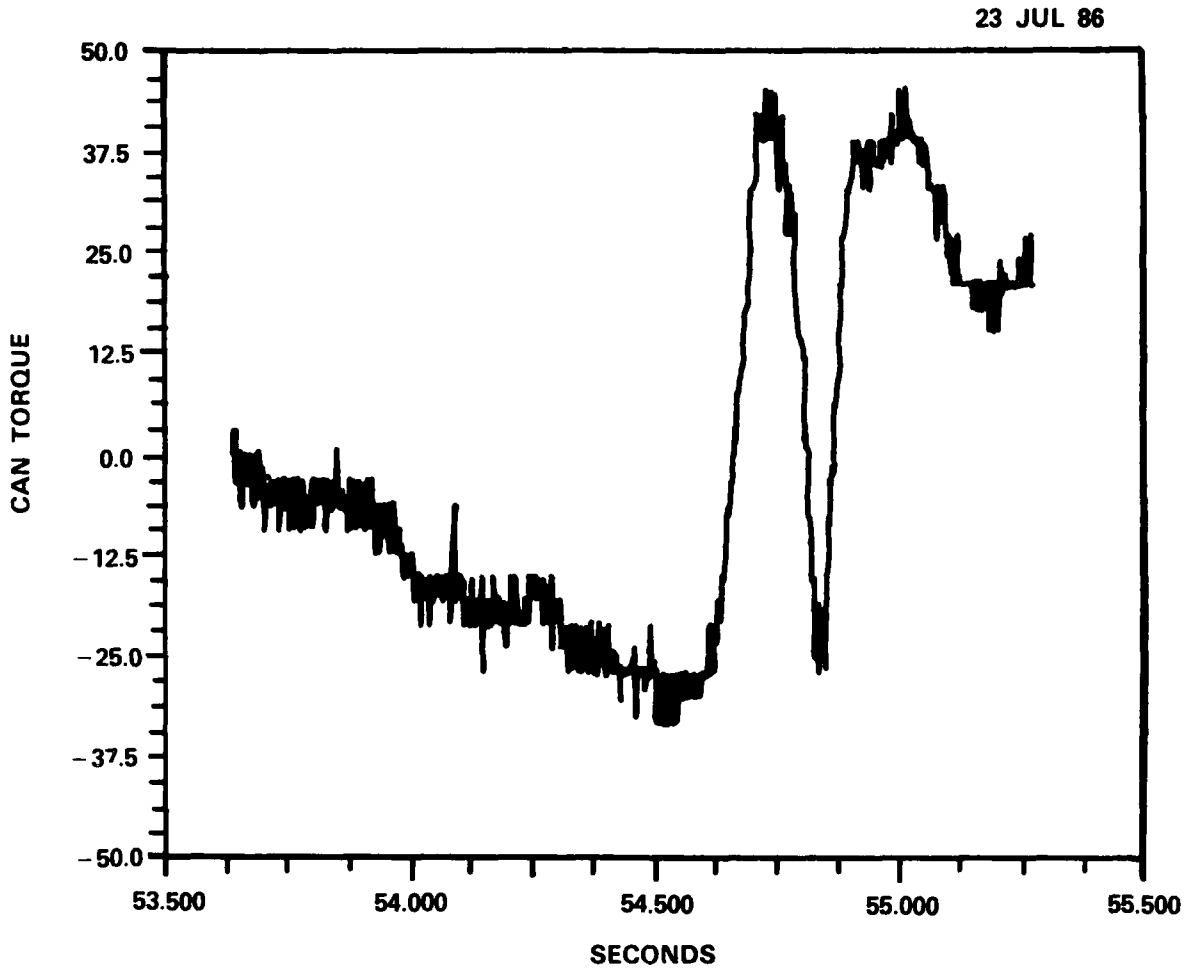

Figure 19

TRACE OF TORQUE FOR FLIGHT # 2

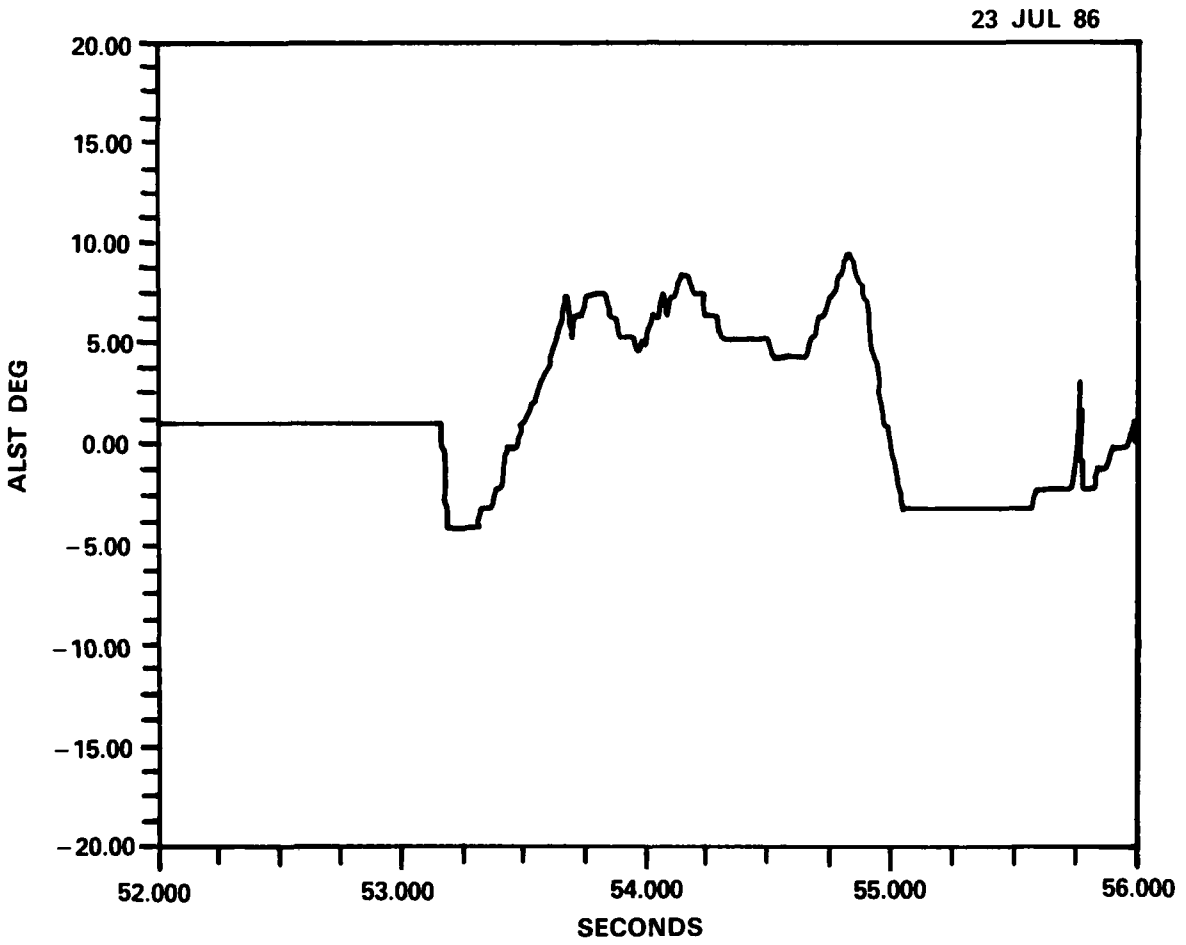

Figure 20

TRACE OF ANGLE OF ATTACK FOR FLIGHT # 2

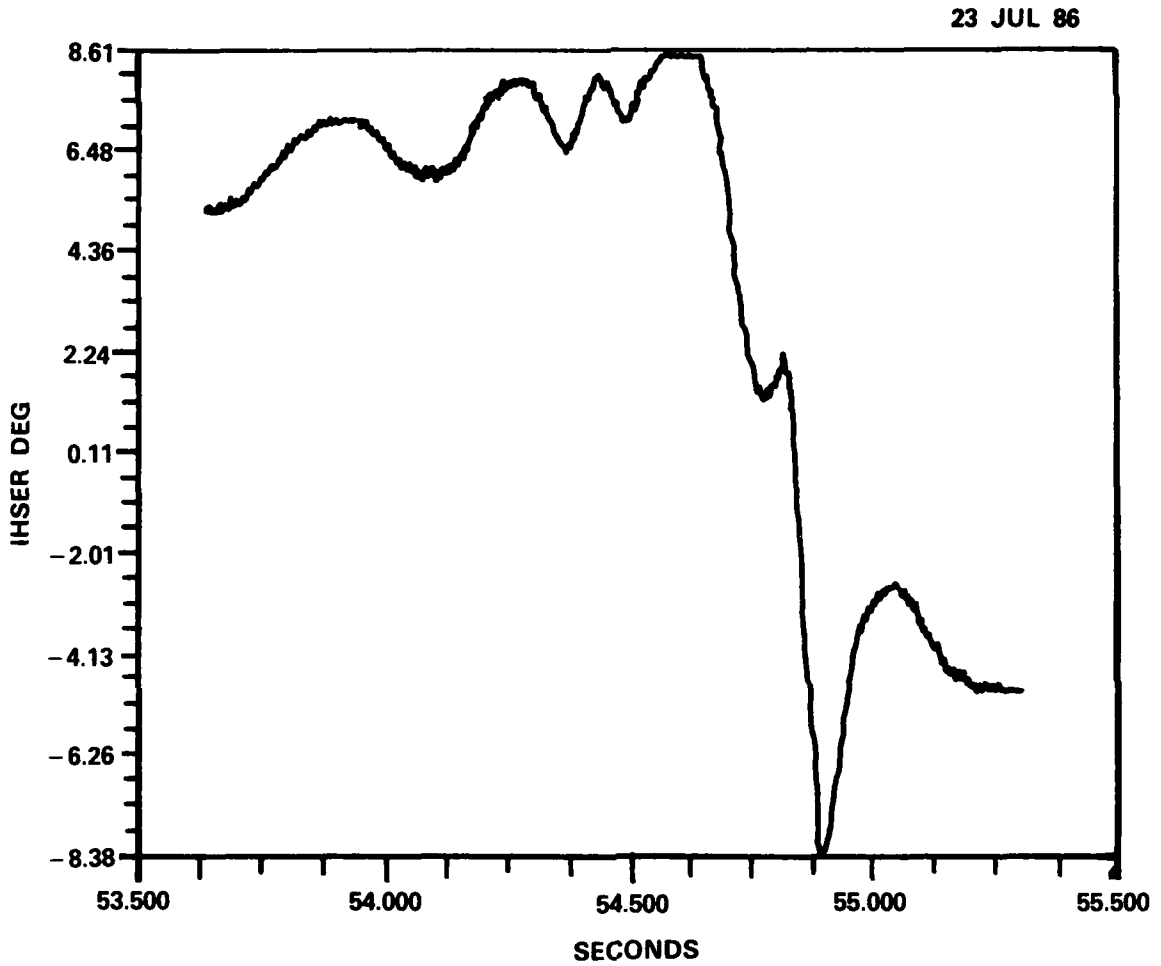

Figure 21

TRACE OF CANARD INCIDENCE ANGLE FOR FLIGHT # 2

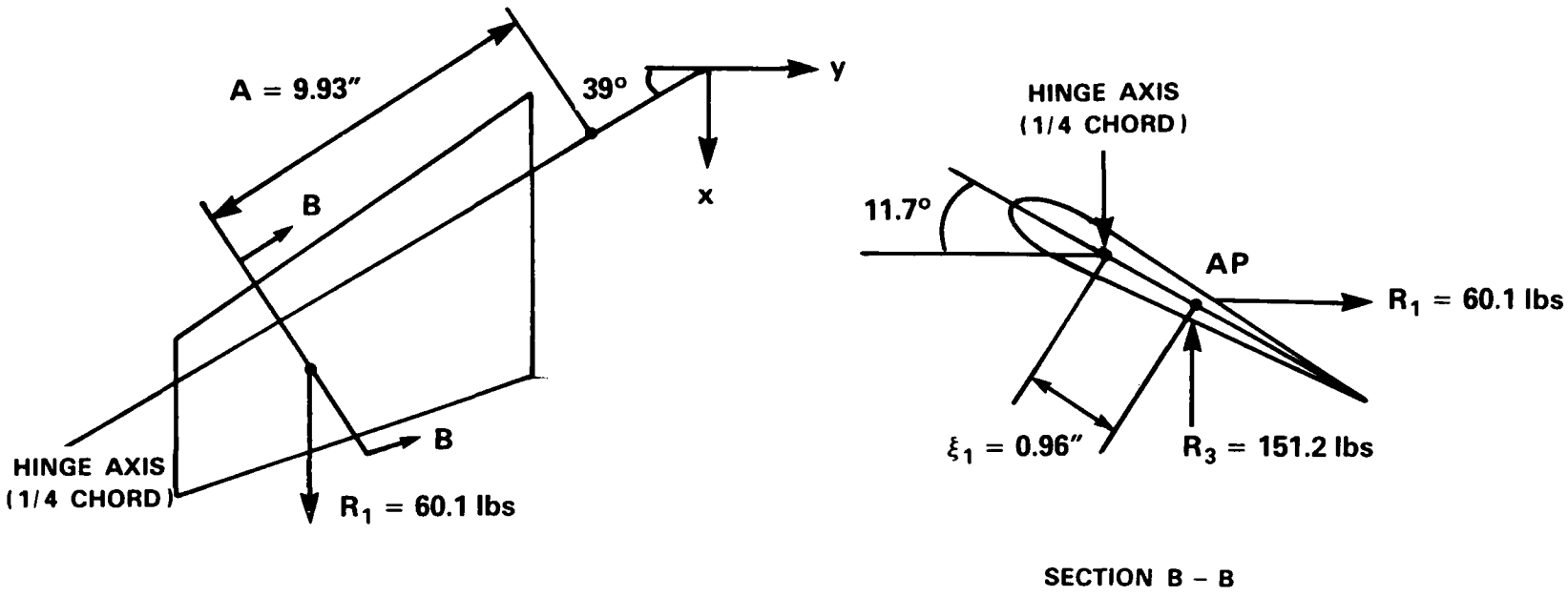

Figure 22

RESULTANT CANARD FORCES

UNCLASSIFIED

This Sheet Security Classification

DOCUMENT CONTROL DATA - R & D

(Security classification of title, body of abstract and indexing annotation must be entered when the overall document is classified)

1 ORIGINATING ACTIVITY

Defence Research Establishment Suffield
Ralston, Alberta TOJ 2NO

2a. DOCUMENT SECURITY CLASSIFICATION

Unclassified

2b. GROUP

3 DOCUMENT TITLE

IN-FLIGHT LOAD MEASUREMENTS OF THE ROBOT-X CANARDS

4 DESCRIPTIVE NOTES (Type of report and inclusive dates)

Suffield Memorandum No. 1191

5 AUTHOR(S) (Last name, first name, middle initial)

Penzes, S.G.

6. DOCUMENT DATE	7a. TOTAL NO. OF PAGES	7b. NO. OF REFS
February 1988	33	6

8a. PROJECT OR GRANT NO.	9a. ORIGINATOR'S DOCUMENT NUMBER(S)
031SE	SM 1191
8b CONTRACT NO.	9b. OTHER DOCUMENT NO.(S) (Any other numbers that may be assigned this document)

10. DISTRIBUTION STATEMENT

UNLIMITED

11. SUPPLEMENTARY NOTES	12. SPONSORING ACTIVITY

13. ABSTRACT

The strain gauge system implemented in one of the ROBOT-X canards is described. The system is designed to measure lift, drag and torque. The description includes design considerations, calibration procedures and data reduction techniques. Data are presented from an early ROBOT-X flight test.

DSIS
79-010

KEY WORDS

ROBOT-X
airframe
canard
stress
stress measurement
aerodynamic load
instrumentation
flight test

INSTRUCTIONS

1. ORIGINATING ACTIVITY: Enter the name and address of the organization issuing the document.

2a. DOCUMENT SECURITY CLASSIFICATION: Enter the overall security classification of the document including special warning terms whenever applicable.

2b. GROUP: Enter security reclassification group number. The three groups are defined in Appendix 'M' of the DRB Security Regulations.

3. DOCUMENT TITLE: Enter the complete document title in all capital letters. Titles in all cases should be unclassified. If a sufficiently descriptive title cannot be selected without classification, show title classification with the usual one-capital-letter abbreviation in parentheses immediately following the title.

4. DESCRIPTIVE NOTES: Enter the category of document, e.g. technical report, technical note or technical letter. If appropriate, enter the type of document, e.g. interim, progress, summary, annual or final. Give the inclusive dates when a specific reporting period is covered.

5. AUTHOR(S): Enter the name(s) of author(s) as shown on or in the document. Enter last name, first name, middle initial. If military, show rank. The name of the principal author is an absolute minimum requirement.

6. DOCUMENT DATE: Enter the date (month, year) of Establishment approval for publication of the document.

7a. TOTAL NUMBER OF PAGES: The total page count should follow normal pagination procedures, i.e., enter the number of pages containing information.

7b. NUMBER OF REFERENCES: Enter the total number of references cited in the document.

8a. PROJECT OR GRANT NUMBER: If appropriate, enter the applicable research and development project or grant number under which the document was written.

8b. CONTRACT NUMBER: If appropriate, enter the applicable number under which the document was written.

9a. ORIGINATOR'S DOCUMENT NUMBER(S): Enter the official document number by which the document will be identified and controlled by the originating activity. This number must be unique to this document.

9b. OTHER DOCUMENT NUMBER(S): If the document has been assigned any other document numbers (either by the originator or by the sponsor), also enter this number(s).

10. DISTRIBUTION STATEMENT: Enter any limitations on further dissemination of the document, other than those imposed by security classification, using standard statements such as:

(1) "Qualified requesters may obtain copies of this document from their defence documentation center."

(2) "Announcement and dissemination of this document is not authorized without prior approval from originating activity."

11. SUPPLEMENTARY NOTES: Use for additional explanatory notes.

12. SPONSORING ACTIVITY: Enter the name of the departmental project office or laboratory sponsoring the research and development. Include address.

13. ABSTRACT: Enter an abstract giving a brief and factual summary of the document, even though it may also appear elsewhere in the body of the document itself. It is highly desirable that the abstract of classified documents be unclassified. Each paragraph of the abstract shall end with an indication of the security classification of the information in the paragraph (unless the document itself is unclassified) represented as (TS), (S), (C), (R), or (U).

The length of the abstract should be limited to 20 single-spaced standard typewritten lines, 7½ inches long.

14. KEY WORDS: Key words are technically meaningful terms or short phrases that characterize a document and could be helpful in cataloging the document. Key words should be selected so that no security classification is required. Identifiers, such as equipment model designation, trade name, military project code name, geographic location, may be used as key words but will be followed by an indication of technical context.

END

DATE

FILMED

6-1988

DTIC